




^{99m}Tc Bone-Avid Tracer Cardiac Scintigraphy: Role in Noninvasive Diagnosis of Transthyretin Cardiac Amyloidosis

Yiu Ming Khor, MBBS, MMed • Sarah A. M. Cuddy, MB, BCh, BAO • Vasvi Singh, MD • Rodney H. Falk, MD • Marcelo F. Di Carli, MD • Sharmila Dorbala, MD, MPH

From the Department of Nuclear Medicine and Molecular Imaging, Singapore General Hospital, Singapore (Y.M.K.); Division of Nuclear Medicine and Molecular Imaging, Department of Radiology (Y.M.K., V.S., M.F.D.C., S.D.), Cardiac Amyloidosis Program, Division of Cardiology, Department of Medicine (S.A.M.C., R.H.F., S.D.), and CV Imaging Program, Cardiovascular Division and Department of Radiology (S.A.M.C., V.S., M.F.D.C., S.D.), Brigham and Women's Hospital and Harvard Medical School, 70 Francis St, Boston, MA 02115; and Midwest Heart and Vascular Specialists, HCA Midwest Health, Kansas City, Mo (V.S.). Received May 16, 2022; revision requested June 27; revision received August 11; accepted September 15. **Address correspondence to** S.D. (email: sdorbala@bwh.harvard.edu).

Supported by the National Institutes of Health (grants HL 130563 [R.H.F.]; and HL 130563, HL 150342, K24 HL157648, AHA19SRG34950011, and 16CSA28880004 [S.D]).

Conflicts of interest are listed at the end of this article.

Radiology 2023; 306(2):e221082 • <https://doi.org/10.1148/radiol.221082> • Content codes:   

Transthyretin cardiac amyloidosis (ATTR-CA) is an overlooked cause of heart failure, with substantial morbidity and mortality. The emergence of several novel therapies has fueled the interest in early and accurate diagnosis of ATTR-CA so that potentially life-saving pharmacologic therapy can be administered in a timely manner. The most promising imaging modality and biomarker is SPECT imaging with technetium ^{99m}Tc -radiolabeled bone-seeking tracers, which have high specificity in the diagnosis of ATTR-CA, potentially obviating biopsy. In this article, the authors provide a focused review on the use of ^{99m}Tc pyrophosphate (PYP), 3,3-diphosphono-1,2-propanodicarboxylic acid (DPD), and hydroxymethylene diphosphonate (HMDP) for diagnosis of ATTR-CA, present a systematic approach to interpretation of the scans, and highlight several common pitfalls to illustrate important diagnostic principles for accurate interpretation of these images. The authors indicate when to use endomyocardial biopsy for the diagnosis of cardiac amyloidosis and conclude with a section on quantitation of ^{99m}Tc -PYP/DPD/HMDP imaging.

© RSNA, 2022

Over the last 5 years, nuclear cardiology has witnessed tremendous growth in the use of technetium ^{99m}Tc bone-avid tracer cardiac scintigraphy for clinical and research applications. Its substantial clinical value for evaluation of patients with heart failure with preserved ejection fraction (HFpEF) has motivated many hospitals to start cardiac amyloidosis imaging programs. However, experience with performance, interpretation, and reporting of ^{99m}Tc bone-avid tracer cardiac scintigraphy remains limited. High-quality scan acquisition, accurate interpretation, and definitive reporting are critical for realization of the full potential of this modality. This review will provide an overview of cardiac amyloidosis, summarize the emerging literature on bone-avid tracer cardiac scintigraphy, and illustrate a step-by-step approach to accurate interpretation and reporting of ^{99m}Tc bone-avid tracer cardiac scintigraphy findings.

Cardiac Amyloidosis

Amyloidoses are protein misfolding disorders characterized by extracellular deposition of insoluble amyloid fibrils in various organs, including the heart (1). Amyloid deposits in the myocardium expand the extracellular space, increase myocardial mass, impair diastolic and systolic function, and result in restrictive heart failure (2). The most common forms of cardiac amyloidosis result from misfolded immunoglobulin light chain (AL) or transthyretin (ATTR) proteins and are thus referred to as AL cardiac amyloidosis and ATTR cardiac amyloidosis (ATTR-CA), respectively (1).

AL amyloidosis is caused by a plasma cell dyscrasia. Cardiac involvement, if untreated, is highly fatal, with

a median survival of less than 12 months (3). With successful anti-plasma cell therapies, including daratumumab (a monoclonal CD38-targeting antibody), superior survival and organ response have been reported (4). Therefore, early and accurate diagnosis is crucial to improve outcomes in AL amyloidosis.

There are two forms of ATTR amyloidosis. One is a hereditary form caused by an autosomal dominant variant in the ATTR gene (hereditary ATTR [ATTR_v] amyloidosis; *v* for variant ATTR). Patients with ATTR_v amyloidosis typically present after 30 years of age (age of symptom onset is determined by the type of variant), with predominantly neuropathic, cardiomyopathic, or mixed manifestations (5). The other, more common form of ATTR amyloidosis, called wildtype ATTR cardiac amyloidosis (ATTR_{wt}-CA), is related to aging and other yet unknown pathophysiologic insults (5). Patients with ATTR_{wt}-CA are predominantly men over age 70 years and often present with heart failure. After the onset of heart failure, median survival of patients with ATTR_{wt}-CA is 4–5 years (6). Until recently, a biopsy was required to diagnose ATTR-CA; because of the low yield of fat pad biopsy (15% for wildtype ATTR and 45% for ATTR_v) (7), endomyocardial biopsy was often performed. Advances in imaging have transformed the evaluation of patients with cardiac amyloidosis, and endomyocardial biopsy is now reserved for challenging cases.

Imaging Evaluation of HFpEF in Older Adults

Suspicion of cardiac amyloidosis in a patient with heart failure is based on typical echocardiographic and/or car-

Abbreviations

AL = light chain, ATTR = transthyretin, ATTR-CA = ATTR cardiac amyloidosis, ATTRv = hereditary ATTR, ATTRwt-CA = wildtype ATTR cardiac amyloidosis, DPD = 3,3-diphosphono-1,2-propanodicarboxylic acid, H/CL ratio = heart-to-contralateral lung uptake ratio, HFpEF = heart failure with preserved ejection fraction, HMDP = hydroxymethylene diphosphonate, PYP = pyrophosphate, ROI = region of interest, ^{99m}Tc = technetium 99m

Summary

This article provides a focused review of transthyretin cardiac amyloidosis and a stepwise approach to accurately and definitively diagnosing it using technetium 99m pyrophosphate, 3,3-diphosphono-1,2-propanodicarboxylic acid, or hydroxymethylene diphosphonate cardiac scintigraphy.

Essentials

- Over the last 5 years, nuclear cardiology has witnessed tremendous growth in the use of technetium 99m (^{99m}Tc) bone-avid tracer cardiac scintigraphy for clinical and research applications.
- A seminal publication confirmed the high diagnostic accuracy of ^{99m}Tc pyrophosphate (PYP), 3,3-diphosphono-1,2-propanodicarboxylic acid (DPD), and hydroxymethylene diphosphonate (HMDP) imaging: In patients with heart failure and typical imaging features of infiltrative heart disease, after exclusion of light chain (AL) amyloidosis, grade 2 or grade 3 myocardial uptake at ^{99m}Tc-PYP/DPD/HMDP imaging is nearly 100% specific for transthyretin cardiac amyloidosis (ATTR-CA).
- A common error in the interpretation of ^{99m}Tc-PYP/DPD/HMDP scans is mistaking tracer activity in the blood pool for tracer uptake by the myocardium, which can be avoided by using SPECT and SPECT/CT.
- A missed or delayed diagnosis of AL amyloidosis is likely fatal; hence, a monoclonal process must be excluded with serum/urine immunofixation electrophoresis and serum free AL assay before a diagnosis of ATTR-CA can be made based on a positive ^{99m}Tc-PYP/DPD/HMDP scan.
- The planar heart-to-contralateral lung uptake (H/CL) ratio is prone to errors and should be used solely to diagnose ATTR-CA at bone-avid tracer cardiac scintigraphy. In our clinical practice, we omit the H/CL ratio and report the visual impression based on SPECT/CT images at 2–3 hours after tracer injection.

diac MRI features (8): increased ventricular wall thickness, increased myocardial mass, abnormal global longitudinal strain with apical sparing, characteristic alterations in gadolinium kinetics, diffuse late gadolinium enhancement, and expansion of the extracellular volume (2). However, cardiac MRI structural and functional imaging features are not specific for amyloidosis and cannot be used to identify amyloidosis at early stages or distinguish the AL and ATTR forms of cardiac amyloidosis (2). Although cardiac uptake of bone-avid tracers has been known since the early 1980s to represent cardiac amyloidosis (9), multiple studies reported variable diagnostic sensitivity, probably because patients with both AL and ATTR forms of cardiac amyloidosis were included in these studies. More than a decade ago, researchers recognized that these tracers provide a highly sensitive signal for ATTR-CA but not for AL cardiac amyloidosis (10). With this new knowledge, subsequent studies focused on diagnosing ATTR-CA. Multiple studies using bone-avid tracer cardiac scintigraphy have confirmed its very high specificity (nearly 100%), allowing noninvasive diagnosis without endomyocardial biopsy (11,12).

Noninvasive Diagnosis of ATTR-CA without Biopsy

Currently, the most established molecular imaging modality for diagnosis of ATTR-CA is scintigraphy with ^{99m}Tc-radiolabeled bone-seeking tracers that are bisphosphonate derivatives, namely ^{99m}Tc pyrophosphate (PYP), ^{99m}Tc 3,3-diphosphono-1,2-propanodicarboxylic acid (DPD), and ^{99m}Tc hydroxymethylene diphosphonate (HMDP). Multiple single-center studies have shown high diagnostic accuracy of ^{99m}Tc-PYP/DPD/HMDP for ATTR-CA (11,13). A seminal publication by Gillmore et al (12), which included 1217 patients with suspected amyloidosis from five countries and seven major amyloidosis centers, confirmed the high diagnostic accuracy of ^{99m}Tc-PYP/DPD/HMDP imaging: In patients with heart failure and typical imaging features of infiltrative pathologic abnormalities, after exclusion of AL amyloidosis, grade 2 or grade 3 myocardial uptake (see following section) on ^{99m}Tc-PYP/DPD/HMDP images was nearly 100% specific for ATTR-CA (12).

Mechanism of Myocardial Uptake of Bone-Avid Tracers in Amyloidosis

The mechanism of myocardial uptake of ^{99m}Tc-radiolabeled bone-seeking tracers in ATTR-CA is not fully understood. A probable mechanism is that these tracers bind to the calcium content within the myocardium affected by amyloidosis, akin to their affinity to the calcium in the bones at sites of active bone formation. In the past, ^{99m}Tc-PYP was used as an imaging tool for diagnosis of myocardial infarct because it binds to the calcium deposits in infarcted myocardium, and the uptake correlates with calcium content in the injured and necrotic myocytes (14). Stats and Stone (15) reported greater microcalcification densities in endomyocardial biopsies from patients with ATTR-CA than those with AL cardiac amyloidosis, which might account for the observed preferential binding of these bone-seeking tracers to ATTR-CA compared with AL cardiac amyloidosis. However, fluorine 18 sodium fluoride, a tracer targeting microcalcification, had not shown consistent or significant myocardial uptake in AL amyloidosis or ATTR-CA (16–18). Interestingly, another commonly used ^{99m}Tc bisphosphonate derivative for bone scintigraphy, ^{99m}Tc methyl diphosphate, was not avid for cardiac amyloidosis (19–21). Although case reports had described varying degree of myocardial uptake in ATTR-CA in a small number of patients (22,23), current recommendations do not advocate the use of ^{99m}Tc methyl diphosphate for cardiac amyloidosis due to its very low sensitivity.

^{99m}Tc-PYP/DPD/HMDP Scintigraphy for Risk Assessment in ATTR-CA

Several studies have reported on the utility of ^{99m}Tc-PYP/DPD/HMDP scintigraphy for risk stratification in ATTR-CA. Although abnormal myocardial uptake of ^{99m}Tc-PYP, ^{99m}Tc-DPD, or ^{99m}Tc-HMDP, compared with no uptake, indicated worse prognosis (24,25), there was no difference in prognosis for visually assessed mildly, moderately, or severely abnormal scans (24). On planar images, semiquantitative metrics of heart-to-contralateral lung uptake ratio (H/CL ratio)

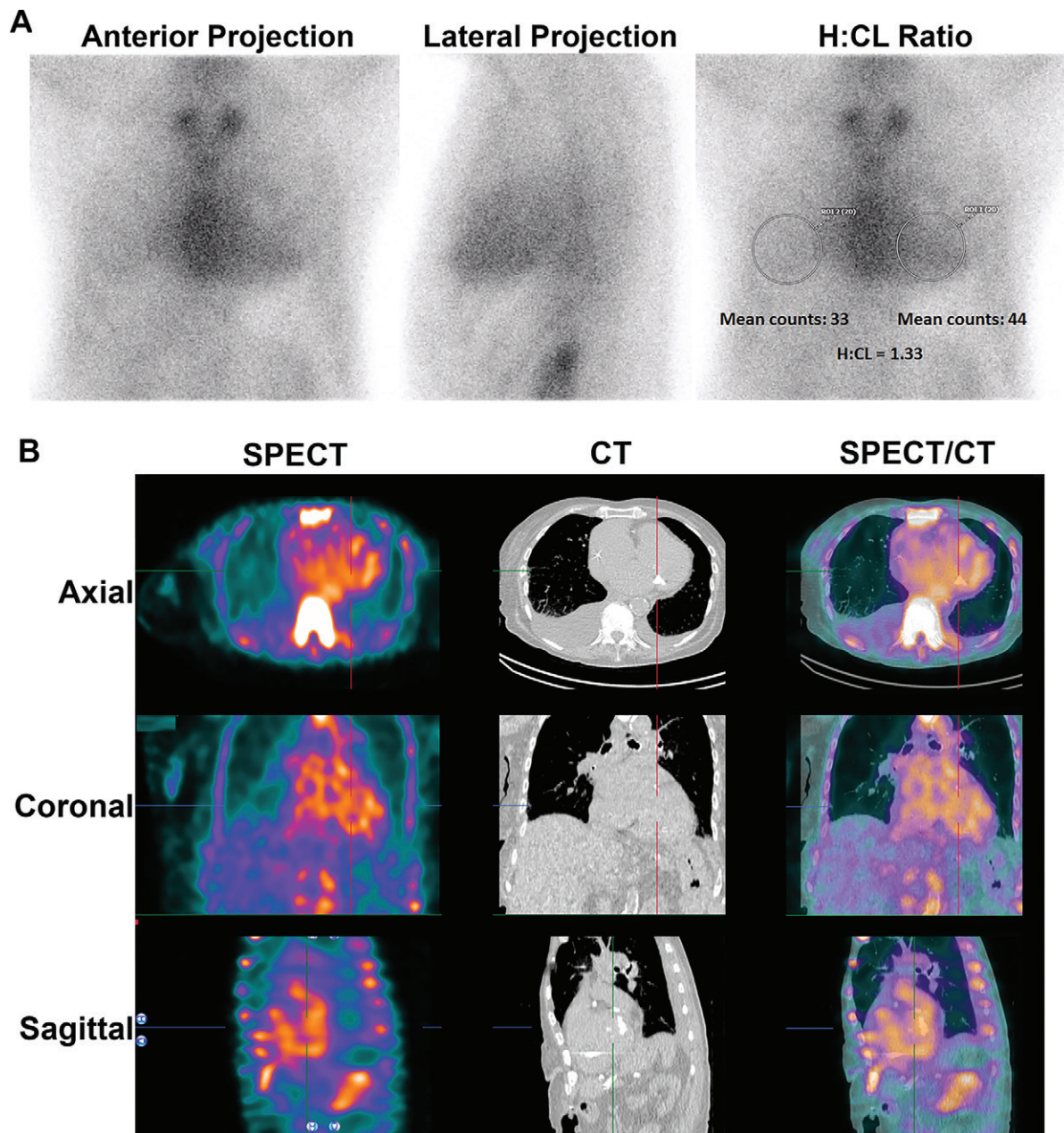


Figure 1: Planar and SPECT/CT technetium ^{99m}Tc pyrophosphate (PYP) images obtained for suspected transthyretin cardiac amyloidosis (ATTR-CA). **(A)** A 77-year-old White man with new onset of symptoms of heart failure underwent ^{99m}Tc -PYP planar scanning. The scan was reported as showing grade 3 myocardial uptake suggestive of ATTR-CA, and the patient was referred to our institution for initiation of tafamidis therapy. A careful review of the ^{99m}Tc -PYP planar images, which were reported to be acquired 1 hour after injection of radiotracer, suggested that tracer activity was concentrated in the blood pool and not in the myocardium because the typical appearance of a central clearing was not evident. Absence of rib uptake of tracer suggested that imaging was performed too early, making the images uninterpretable (see also Fig 2). H/CL = heart-to-contralateral lung uptake ratio, ROI = region of interest, 2D = two-dimensional. **(B)** SPECT/CT imaging at 3 hours is the preferred protocol at our institution, and it clearly demonstrates blood pool activity, with no myocardial ^{99m}Tc -PYP uptake in the rib. A definitive diagnosis of ATTR-CA based on interpretation of ^{99m}Tc -PYP planar images alone is not possible even for experienced readers.

greater than 1.6 (see section “How to Interpret ^{99m}Tc -PYP/DPD/HMDP Images: A Systematic Approach”) (26) and heart-to-whole body ratio greater than 7.5 (25) were associated with worse major adverse event-free survival. Heart-to-whole body ratio was obtained by dividing the counts in the heart by the counts in whole-body image at 3 hours after injection of ^{99m}Tc -DPD (25).

^{99m}Tc -PYP/DPD/HMDP Scintigraphy to Unravel the Prevalence of ATTR-CA in Select at-Risk Cohorts

Autopsy studies revealed that ATTR amyloid deposits are prevalent in older adults, with more than 20% of persons showing evidence of myocardial ATTR amyloid deposition after age 80 years. However, a clinical diagnosis is made in far fewer patients (27). Clinical diagnosis using bone-avid tracer

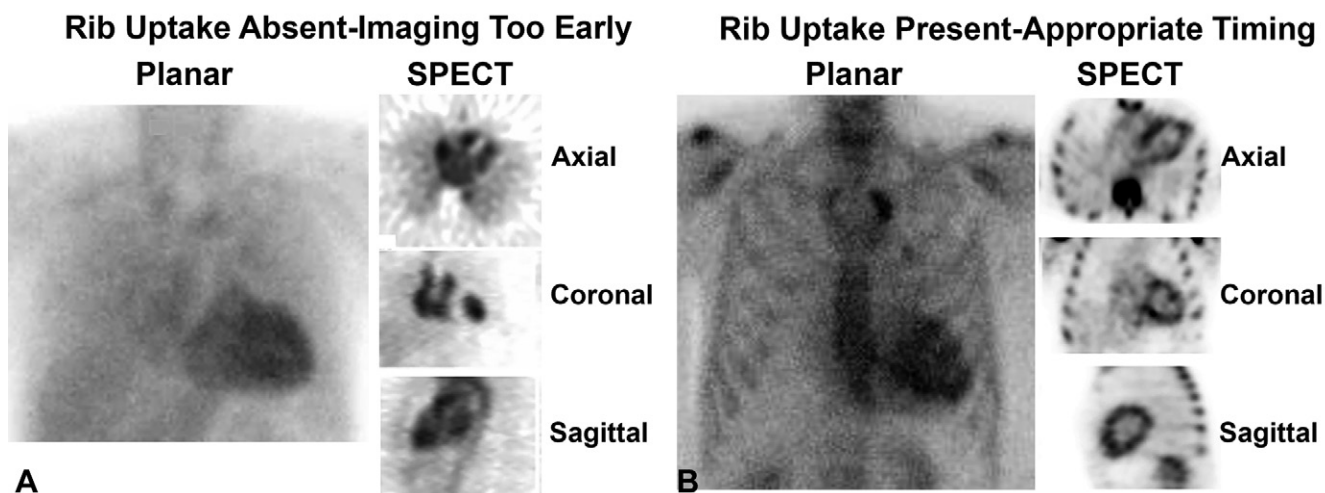


Figure 2: Rib uptake as an indication of appropriate timing of scan acquisition in technetium ^{99m}pyrophosphate cardiac scintigraphy. **(A)** In the early phase shortly after tracer injection, blood pool activity within the heart is expected, while the ribs and other skeletal structures are not clearly visible. The absence of tracer uptake by the ribs is a good indicator that it is too early to interpret the scan, as the tracer is still circulating in the blood pool and has not entered the myocardium or bound to the bones. **(B)** In contrast, late images acquired 3 hours after radiotracer injection clearly show tracer uptake in the ribs. Any tracer uptake in the heart on 3-hour images should raise suspicion for myocardial uptake.

cardiac scintigraphy to screen at-risk populations (without endomyocardial biopsy) has provided new knowledge on the clinical epidemiology of ATTR-CA. In older adults (age >60 years) hospitalized with HFpEF and increased left ventricular wall thickness (>12 mm), ATTR-CA was found in 13%–21% of patients (28–30). ATTR-CA was also identified among patients with severe aortic valve stenosis: 6%–9% of those undergoing surgical aortic valve replacement (31,32), as many as 9%–13% of patients undergoing transcatheter aortic valve replacement (33–37), and nearly 30% of patients with low-flow low-gradient aortic stenosis (35). Finally, in a large community-based screening study, 6.3% of patients over 60 years of age with HFpEF and increased wall thickness had ATTR-CA (38). ^{99m}Tc bone-avid tracer scintigraphy has revealed that ATTR-CA is likely underdiagnosed and affects about 10% of older adults with HFpEF and increased left ventricular wall thickness.

Novel Targeted Therapies for ATTR-CA

Transthyretin protein normally exists in a homotetrameric form. Aging or ATTR gene variants can destabilize the transthyretin tetramer, causing a dissociation into aggregation-prone monomers that form ATTR amyloid fibrils (5). Until 2018, ATTR amyloidosis was untreatable, but three highly effective therapies are now approved by the U.S. Food and Drug Administration. Inotersen (an antisense oligonucleotide inhibitor) (39) and patisiran (a double-stranded small interfering RNA gene-silencing therapy) (40) halt production of variant ATTR protein and are approved for ATTRv neuropathy. Tafamidis (41), an ATTR-stabilizing agent that prevents the breakdown of ATTR, is approved for ATTR cardiomyopathy (wildtype ATTR or ATTRv). Tafamidis was found to be less effective in patients with advanced ATTR-CA (41). Next-generation gene silencers, and even a CRISPR/

Cas9 (42) in vivo gene-editing therapy for treatment of ATTRv amyloidosis, are currently under development. Most of the current ATTR-CA therapies focus on the precursor protein (43), and no approved therapies are directed against the amyloid fibril. One year after ATTR stabilization or silencing therapy in ATTRv amyloidosis, minimal changes in cardiac structure and function were described at echocardiography (44) or cardiac MRI (45), but a 20% reduction in cardiac uptake of bone-avid tracers was described (45). Whether improvement in cardiac uptake of bone-avid tracers represents improvement in myocardial amyloidosis is not known. This is because current treatments target the precursor protein and improvements in cardiac structure and function are small, as they represent natural regression of amyloid. As the mechanism of tracer binding to amyloid is not known, the significance of decrease in myocardial radiotracer uptake after treatment with ATTR silencing therapy is not known. Newer therapies directed at the amyloid fibril are currently under investigation (43). Molecular amyloid imaging is likely to play an important role in identifying candidates for antifibril-based therapies as well as in the assessment of response to therapy.

In summary, we now have the capability for noninvasive, definitive diagnosis of ATTR-CA using widely available ^{99m}Tc bone-avid tracer cardiac scintigraphy. In combination with new and effective disease-modifying therapies, the use of ^{99m}Tc-PYP/DPD/HMDP imaging has dramatically increased worldwide. In the following sections, we focus on interpretation of ^{99m}Tc-PYP/DPD/HMDP imaging, highlight important diagnostic principles, and discuss common pitfalls that confound image interpretation. The images in this article are primarily ^{99m}Tc-PYP scans, but the principles of evaluation and diagnostic performance are similar for all three tracers (^{99m}Tc-PYP, ^{99m}Tc-DPD, and ^{99m}Tc-HMDP) (46).

Table 1: Recommendations on Acquisition Parameters for ^{99m}Tc-PYP/DPD/HMDP Imaging for Cardiac Amyloidosis

Imaging Procedure	Parameter	Recommendation
Preparation	No specific preparation; no fasting required	...
Scan	Rest scan	Required
Dose	370–740 MBq (10–20 mCi) intravenously for ^{99m} Tc-PYP, ^{99m} Tc-DPD, and ^{99m} Tc-HMDP	Recommended
Time between injection and acquisition: ^{99m} Tc-PYP/DPD/HMDP	2 or 3 hours	Recommended
Time between injection and acquisition: ^{99m} Tc-PYP only	1 hour	Optional; if excess blood pool activity is noted on 1-hour images, 3-hour imaging is recommended (see below regarding image type)
General imaging parameters*		
Field of view	Heart	Required
	Chest	Optional for planar
CT attenuation correction	Heart	Recommended (SPECT/CT fusion images helpful to localize tracer uptake in the myocardium)
Image type: planar	Chest	Recommended (1-hour planar-only imaging is not recommended)
Image type: SPECT	Heart	Required
Position	Supine	Required
	Upright	Optional
Energy window	140 keV, 15%–20%	Required
Collimators	Low energy, high resolution	Recommended
Matrix: planar	256 × 256	Recommended
Matrix: SPECT	128 × 128 (at least 64 × 64 is required)	Recommended
Pixel size	3.5–6.5 mm	Recommended
Planar imaging–specific parameters*		
View [†]	Anterior and lateral	Required
Detector configuration	90°	Recommended
Image duration (count-based)	750,000 counts	Recommended
Magnification	×1.46 for large–field of view systems	Recommended
	×1.0 for small–field of view systems	Optional
SPECT imaging–specific parameters*		
Angular range	180°	Required
	360°	Optional
Detector configuration	90°	Recommended
	180°	Optional
Electrocardiogram gating	Off; nongated imaging	Recommended
No. of views/detector	40/32	Recommended
Time per stop	20 seconds/25 seconds	Recommended
Magnification	×1.46 (180° angular range)	Recommended
	×1.0 (360° angular range)	

Note.—DPD = 3,3-diphosphono-1,2-propanodicarboxylic acid, HMDP = hydroxymethylene diphosphonate, PYP = pyrophosphate, ^{99m}Tc = technetium 99m. Adapted, with permission, from reference 73.

* Parameters for sodium iodide SPECT scanners.

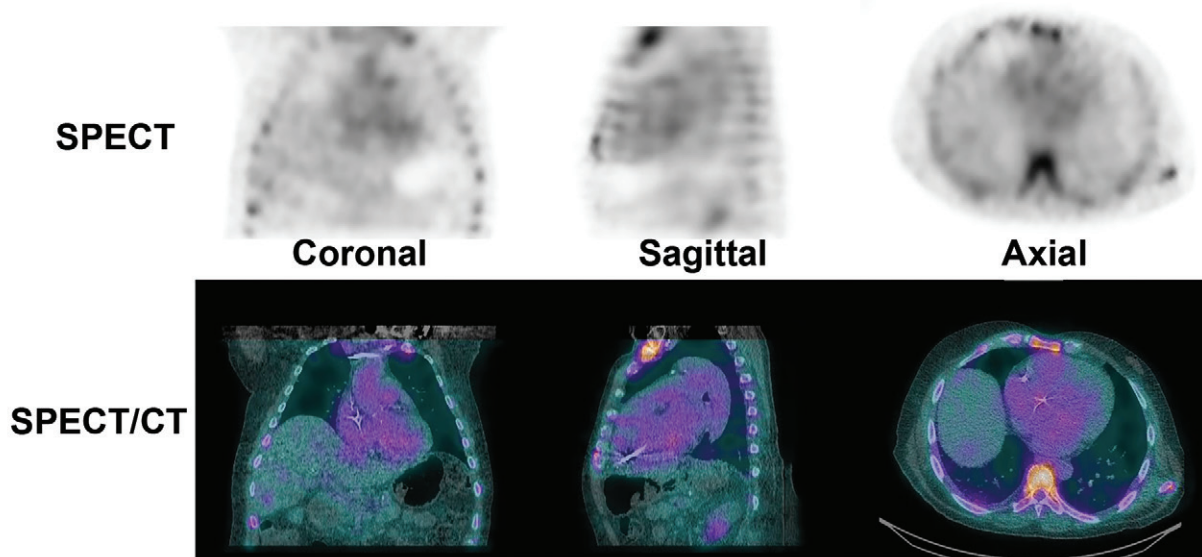
[†] Anterior and lateral views are obtained at the same time; lateral planar views or SPECT imaging may help separate sternal from myocardial uptake.

Clinical Vignette

A 77-year-old man with HFpEF was referred to our hospital for management of newly diagnosed ATTR-CA. His echocardiogram showed normal left ventricular ejection fraction and increased left ventricular wall thickness with restrictive filling characteris-

tics. Global longitudinal strain was reduced at –14.8%. His troponin-T level was 28 ng/L (reference range: 0–14 ng/L), and his *N*-terminal pro-B-type natriuretic peptide level was 602 pg/mL (reference level: less than 450 pg/mL). He underwent ^{99m}Tc-PYP scintigraphy at an outside hospital, and the scan was interpreted as

A Blood Pool Activity



B Myocardial Activity

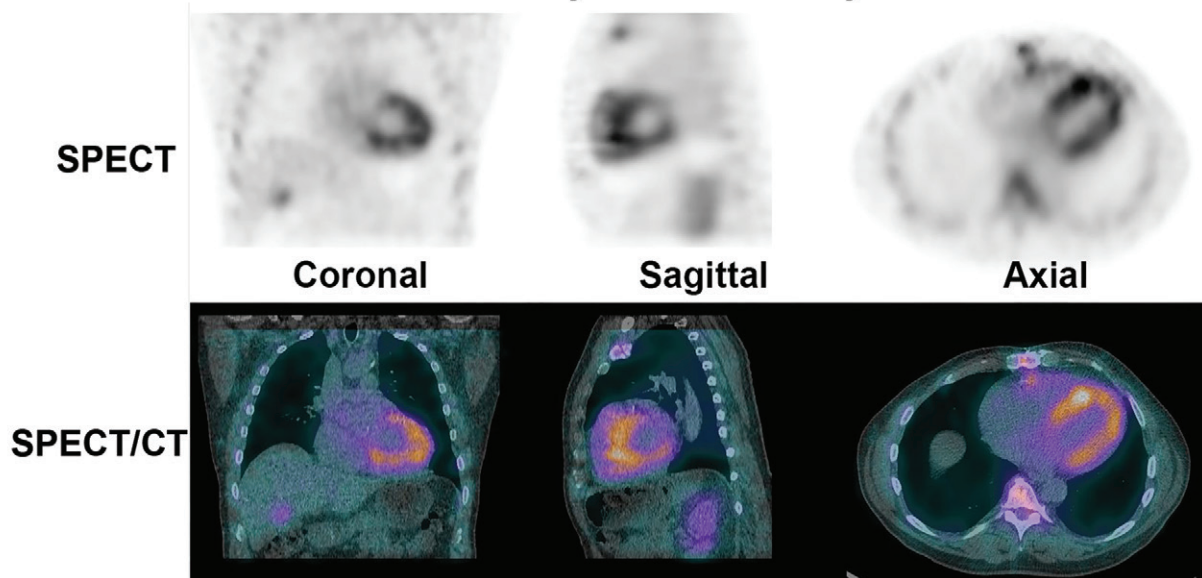


Figure 3: SPECT and SPECT/CT to distinguish myocardial technetium ^{99m}pyrophosphate uptake from blood pool activity. **(A)** On SPECT and SPECT/CT images, tracer activity in the blood pool has an amorphous appearance that is not clearly separable from the mediastinum. **(B)** True-positive tracer uptake by the myocardium is characterized by a U shape or horseshoe shape on the axial and coronal planes and a donut shape on the sagittal plane.

showing grade 3 myocardial uptake (Fig 1A) that was suggestive of ATTR-CA. His serum free AL levels and serum and urine immunofixation electrophoresis findings were normal. He was referred to our hospital for further management with a view to initiate pharmacologic treatment with an ATTR stabilizer.

A careful review of the ^{99m}Tc-PYP planar images, which were acquired 1 hour after radiotracer injection, suggested tracer activity was concentrated in the blood pool and not in the myocardium. To confirm, we repeated the ^{99m}Tc-PYP scanning using SPECT/CT at 3 hours after tracer injection (Fig 1B). The images confirmed blood pool activity with no myocardial ^{99m}Tc-PYP uptake. Diagnostically, the onset of his heart failure symptoms

coincided with the new diagnosis of atrial fibrillation, suggesting the primary cause of his symptoms was most likely atrial fibrillation superimposed on a stiff ventricle from a combination of diabetes, prior coronary artery disease, and hypertension.

How to Acquire ^{99m}Tc-PYP/DPD/HMDP Images

Guidelines on image acquisition and scan protocols for ^{99m}Tc-PYP/DPD/HMDP studies based on expert consensus are described in Table 1. We highlight that the recommended time of imaging is 2–3 hours after injection of ^{99m}Tc-PYP/DPD/HMDP; imaging at 1 hour is optional for laboratories with vast experience with both 1-hour and 3-hour ^{99m}Tc-PYP imaging. SPECT, or

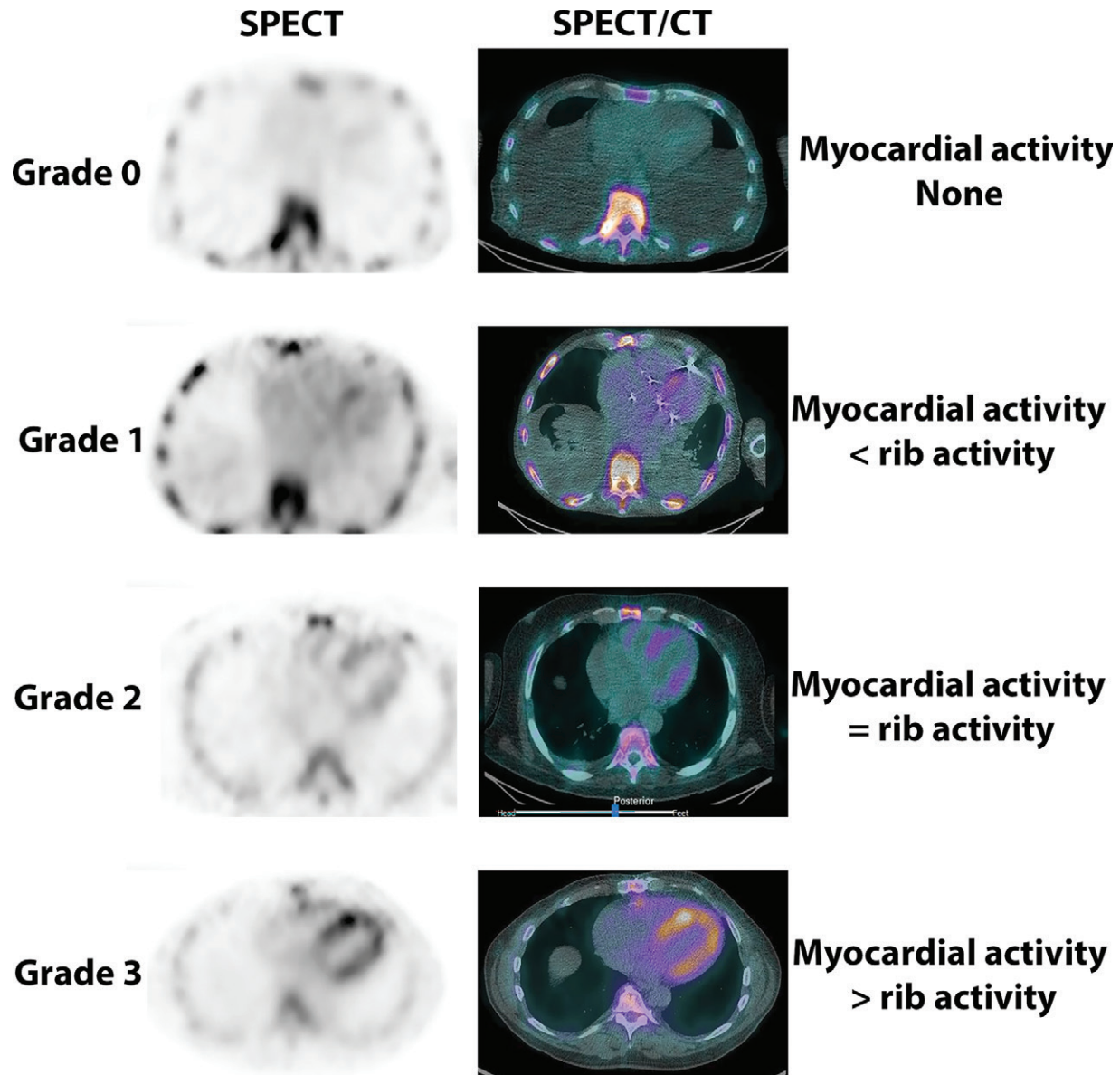


Figure 4: Visual grading of technetium ^{99m}Tc pyrophosphate (PYP) cardiac images. ^{99m}Tc -PYP axial SPECT images (left column) and SPECT/CT images (right column) demonstrate no myocardial uptake of PYP (grade 0) and myocardial tracer uptake less than rib uptake (grade 1), equal to rib uptake (grade 2), and greater than rib uptake (grade 3).

preferably SPECT/CT, is required, as it is the only definitive way to visualize ^{99m}Tc -PYP/DPD/HMDP uptake in the myocardium and differentiate it from blood pool activity (47).

How to Interpret ^{99m}Tc -PYP/DPD/HMDP Images: A Systematic Approach

Step 1: Perform Quality Control

As with any other radiopharmaceutical agent, strict compliance with quality control regulations for radiochemical purity is necessary before intravenous administration of ^{99m}Tc -PYP/DPD/HDP. Dissociation of ^{99m}Tc -PYP can occur after prolonged standing (more than 6 hours) or a change in pH, where free dissociated ^{99m}Tc pertechnetate is seen as unexpected activity in the thyroid and stomach (48). Interpretation of the planar images becomes

challenging due to proximity of the stomach to the heart, but this may be overcome on SPECT images. Excessive free ^{99m}Tc pertechnetate may result in false-negative scans. Laboratories that are new to radiolabeling ^{99m}Tc -PYP should be aware that the stannous PYP kit is not only used for bone and myocardial imaging but can also be used for gated blood pool imaging if reconstituted and administered differently. Both preparation methods are detailed in the product package insert, and confusing one for the other will result in a radiolabeled product that remains in the blood pool with no localization to the myocardium or bone.

Step 2: Confirm the Presence of Rib Uptake as a Check for Appropriate Timing of Scan Acquisition

An important concern is mistaking tracer activity in the blood pool for tracer uptake by the myocardium on planar images. A

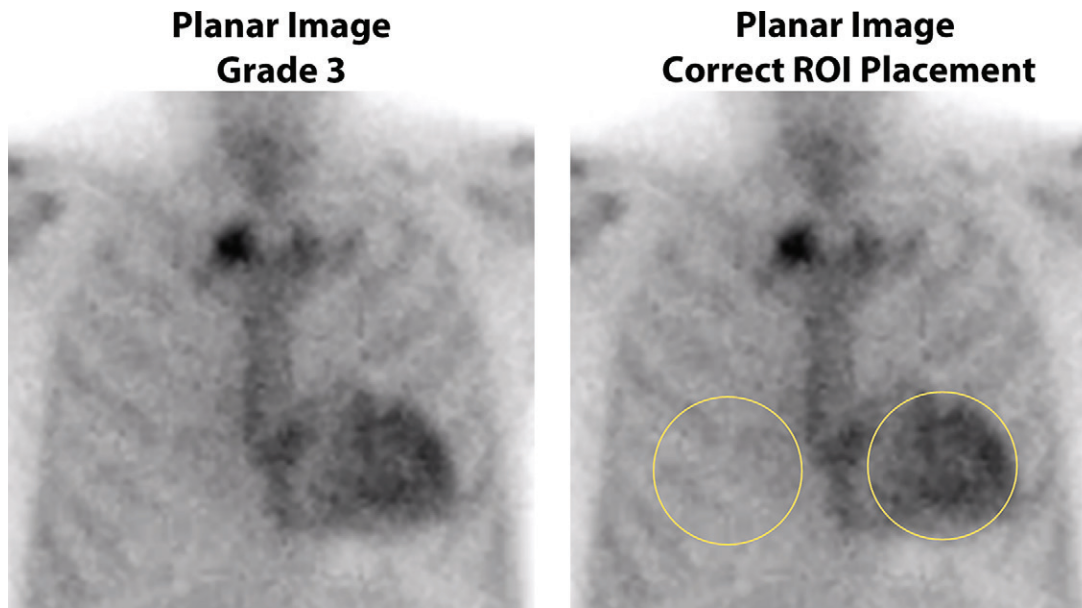


Figure 5: Semiquantitative method of heart-to-contralateral lung uptake ratio (H/CL ratio) uptake ratio on planar imaging at 1 hour after tracer injection. Anterior planar images acquired 1 hour after injection of technetium 99m pyrophosphate show grade 3 myocardial tracer uptake. Correct placement of regions of interest (ROIs) for the derivation of H/CL ratio is shown: The “heart” ROI should be drawn over the entire myocardium, and the “contralateral chest” ROI should be of the same size and mirrored over the contralateral chest on planar imaging at 1 hour. The ROI should be positioned to minimize overlap with sternal or focal rib uptake and maximize coverage of the heart without including adjacent lung. The H/CL ratio is optional and should only be reported if myocardial activity is noted on SPECT images.

common reason for this is performing the scan too early after injection of radiotracer. The absence of tracer uptake by the ribs, especially with ^{99m}Tc-PYP, is an indicator that images were obtained too early for an interpretable scan (Fig 2A). When scans from a later time point are obtained, they clearly demonstrate symmetric tracer uptake in the bones (Fig 2B). Any tracer uptake in the region of the heart on planar images should raise suspicion for myocardial uptake and must be confirmed with use of SPECT. Substantial soft-tissue uptake of ^{99m}Tc-DPD, predominantly in skeletal muscles, has been reported in patients with ATTR-CA; this can sometimes attenuate visualization of radiotracer uptake by the bone (49).

Step 3: Distinguish Myocardial ^{99m}Tc-PYP Uptake from Blood Pool Activity

A common misinterpretation of ^{99m}Tc-PYP cardiac images is mistaking tracer activity in the blood pool for tracer uptake by the myocardium, as illustrated in the case vignette. SPECT, and SPECT/CT if available, can be used to confirm ^{99m}Tc-PYP uptake in the myocardium and differentiate it from blood pool radioactivity. It is important for imaging physicians to be familiar with the appearance of blood pool activity on SPECT images (Fig 3).

Step 4: Interpret Myocardial Uptake: Visual Assessment and Grading of ^{99m}Tc-PYP Images

^{99m}Tc-PYP/DPD/HMDP chest images are optimally reviewed in transaxial, sagittal, and coronal projections. Reorientation of the images into cardiac projections can be challenging in negative scans, and in positive scans, myocardial activity may be scaled higher when using the cardiac projections alone. When

^{99m}Tc-PYP accumulates in the myocardium, the scan appearance should be similar to a normal myocardial perfusion scan, with high signal intensity in the myocardium and minimal, if any, activity in the blood pool. An inverse gray scale or any linear color scale can be used for SPECT interpretation. For SPECT/CT fusion images, CT is displayed in gray scale and SPECT in color scale.

Once tracer uptake is ascertained to be in the myocardium, the degree of uptake can be categorized using a four-point visual scoring system, which is widely known as the Perugini score (Fig 4). Myocardial uptake of ^{99m}Tc-PYP at 3-hour imaging is graded as follows: grade 0, no myocardial uptake; grade 1, myocardial uptake less than bone uptake; grade 2, myocardial uptake comparable with bone uptake; and grade 3, myocardial uptake more than bone uptake, where bone uptake is defined by tracer uptake by the ribs (11).

In patients with heart failure and typical imaging findings on echocardiographic or cardiac MRI scans, a finding of grade 2 or 3 myocardial uptake in the absence of a monoclonal protein in the serum or urine is nearly 100% specific for ATTR-CA, obviating endomyocardial biopsy (12). A visual score of 0 is not suggestive of ATTR-CA, while a visual score of 1 is equivocal for ATTR-CA (and may represent early ATTR-CA). A visual score of 0–3 can be present in patients with AL cardiac amyloidosis.

Optional Step for Interpretation: Semiquantitative Method of H/CL Ratio at Planar Imaging

The H/CL ratio is defined as the ratio of mean counts obtained in the region of interest (ROI) drawn over the entire cardiac silhouette to the counts within a similar-sized ROI mirrored over

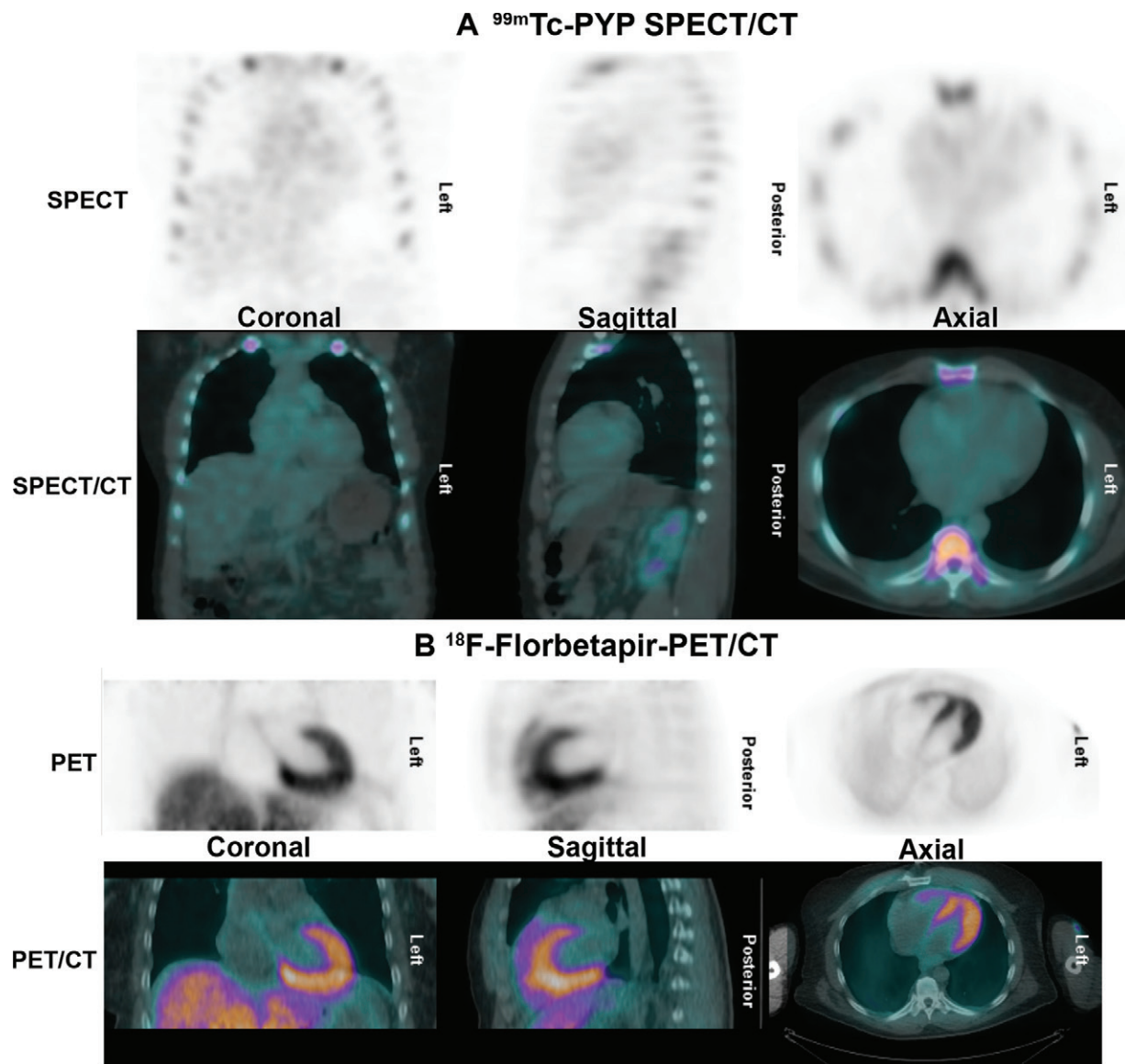


Figure 6: Negative technetium ^{99m}Tc pyrophosphate (PYP) scan in light chain (AL) amyloidosis. A 56-year-old African American man was evaluated with cardiac MRI for symptoms of heart failure. The cardiac MRI findings (not shown) were suggestive of amyloidosis, but **(A)** the ^{99m}Tc -PYP SPECT/CT images show grade 0 uptake. Further evaluation with serum and urine studies as well as bone marrow biopsy confirmed a diagnosis of systemic AL amyloidosis. **(B)** Fluorine 18 (^{18}F) florbetapir PET/CT images acquired as a part of a research study demonstrate diffuse intense myocardial uptake consistent with AL amyloidosis. Amyloid PET tracers may be helpful to identify AL amyloidosis but are currently investigational.

the contralateral lung on planar images (Fig 5). The H/CL ratio is usually concordant with the visual grading at SPECT and is an optional adjunct to support decision-making. An H/CL ratio at 1-hour imaging greater than 1.5 was associated with worse survival (26) and was able to help distinguish ATTR-CA from AL amyloidosis (50). However, scanning 1 hour after injection of ^{99m}Tc -PYP/DPD/HMDP frequently produces images showing high blood pool activity and is not recommended (47). In the presence of high blood pool activity or low contralateral lung activity, as in pleural effusions, the H/CL ratio may be falsely elevated. Care should be taken during the placement of the ROI to avoid overlap with sternal and focal rib uptake as well as the adjacent lung. Common errors include drawing an ROI of a different size, wrong positioning of the ROI over the contralateral lung, or

inclusion of focal rib uptake in the ROI. In some instances, it is acceptable to derive the H/CL ratio by placing an ROI of a different size or at a different site in the contralateral hemithorax to avoid the overlapping tracer uptake. Due to the many limitations, there is no clear added value of the planar H/CL ratio, and in our clinical practice, we omit the H/CL ratio and report solely the visual impression based on the SPECT/CT images at 2–3 hours after tracer injection.

Step 5: Exclude a Monoclonal Process with Serum/Urine Immunofixation Electrophoresis and a Serum Free AL Assay in All Patients with Suspected Cardiac Amyloidosis
Although ^{99m}Tc -PYP/DPD/HMDP scans are less sensitive for AL amyloidosis, with grade 0 uptake seen in nearly 60% of pa-

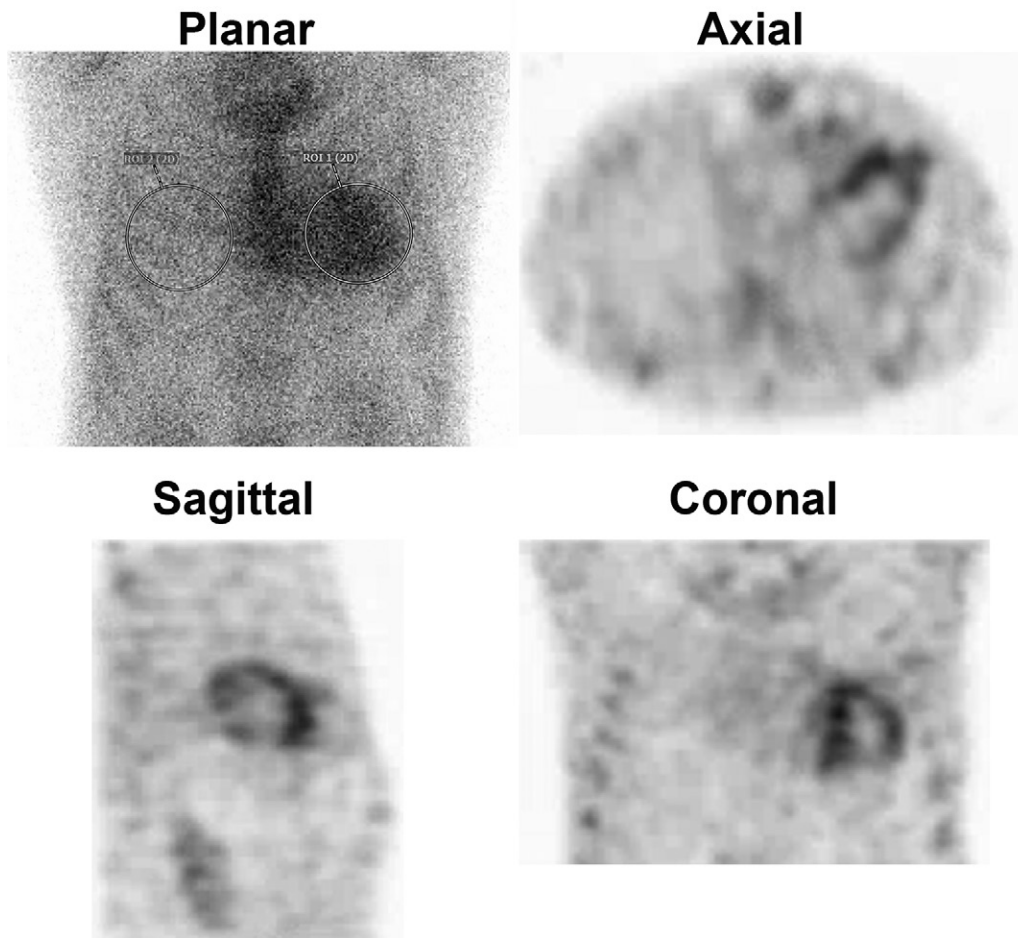


Figure 7: Technetium 99m (^{99m}Tc) pyrophosphate (PYP) scan positive for light chain (AL) amyloidosis. ^{99m}Tc-PYP planar images in a 67-year-old White man with suspected amyloidosis were strongly positive, with grade 3 uptake and an elevated heart-to–contralateral lung uptake ratio of 1.54. Myocardial uptake was confirmed on axial, sagittal, and coronal SPECT images. However, subsequent investigations confirmed the diagnosis of AL amyloidosis. Intense myocardial ^{99m}Tc-PYP uptake can be seen in more than 20%–30% of patients with AL amyloidosis; therefore, a monoclonal process must be excluded by means of serum/urine immunofixation electrophoresis and a serum free AL assay before a diagnosis of transthyretin cardiac amyloidosis is made based on a positive ^{99m}Tc-PYP scan. ROI = region of interest, 2D = two-dimensional.

tients (Fig 6), more than 40% of patients with AL amyloidosis can demonstrate myocardial uptake of these tracers (Fig 7), with intense uptake (grade 2 or 3) in 20%–30% (12). If untreated, AL amyloidosis is a highly fatal disease with a median survival of less than 12 months, but outcomes are much better when it is diagnosed early and treated without delay (3). For these reasons, serum/urine immunofixation electrophoresis and serum free AL assay are recommended in all patients with suspected amyloidosis. Immunofixation is essential because the level of paraprotein in AL amyloidosis is often very low and is detectable with use of routine electrophoresis in only 50% of patients with AL amyloidosis (51). Therefore, a monoclonal process must be excluded with serum/urine immunofixation electrophoresis and serum free light chain assay before the confirmation or exclusion of a diagnosis of ATTR-CA based on a ^{99m}Tc-PYP/DPD/HMDP scan. In practice, patients referred for ^{99m}Tc-PYP/DPD/HMDP scans often have not had a complete evaluation for AL amyloidosis. If a patient has had any positive evaluation for AL amyloidosis (ie, serum/urine immunofixation electrophoresis or

serum free AL assay), then involved organ biopsy, cardiac MRI, or an endomyocardial biopsy may be preferred over ^{99m}Tc-PYP/DPD/HMDP scintigraphy. Coexistent monoclonal gammopathy can be found in up to 40% of patients with ATTRwt-CA (52), and such patients require expert evaluation.

Step 6: Review for Physiologic Tracer Distribution and Extracardiac Tracer Activity

As with all imaging modalities, physicians must exercise due diligence during interpretation and look beyond the organ of interest to examine the entire imaged volume for incidental, potentially actionable findings. Physiologic distribution of ^{99m}Tc-PYP/DPD/HMDP includes symmetric bone uptake, with activity in the bladder, kidney, and soft tissues (53). Asymmetric or focal increased bony tracer uptake is usually attributed to benign causes, such as rib fractures and degenerative changes, but may warrant further evaluation if a sinister pathologic origin is suspected, such as bone metastasis, metabolic bone disease, or Paget disease (Fig 8) (48). Extracardiac ^{99m}Tc-PYP activity has been reported, most

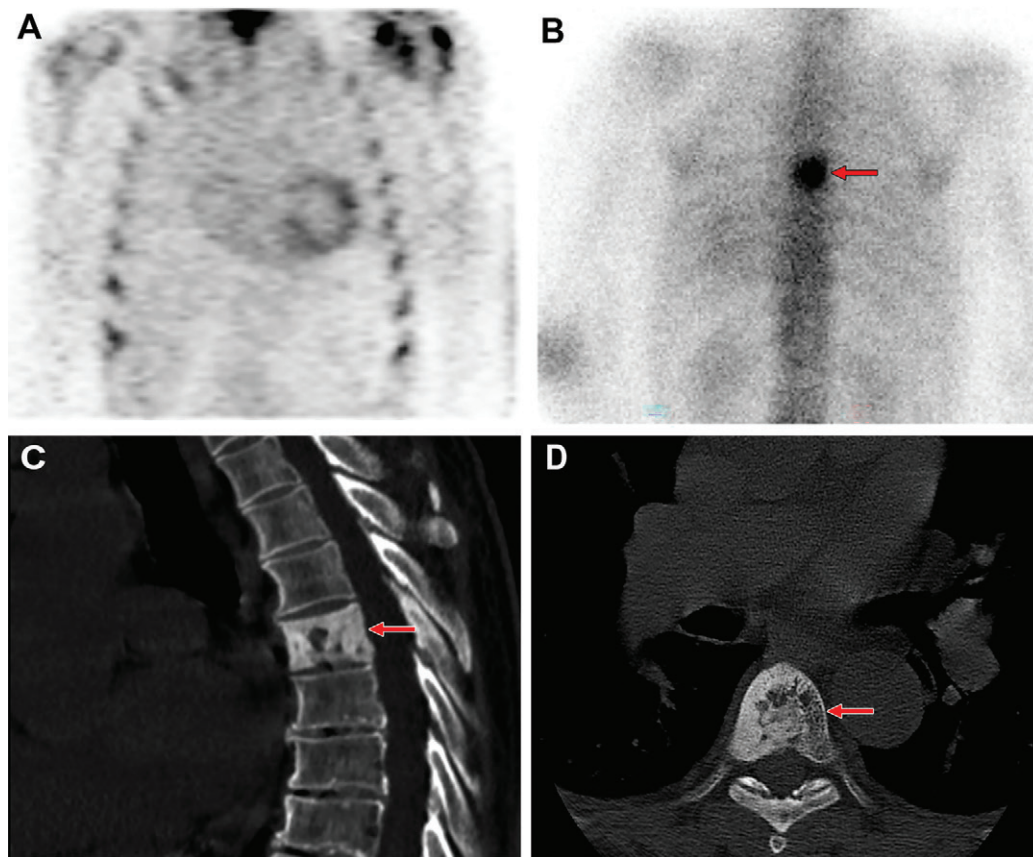


Figure 8: Review of technetium ^{99m}Tc pyrophosphate (PYP) images for extracardiac tracer activity. **(A)** ^{99m}Tc -PYP SPECT chest images in a 76-year-old White man with suspected cardiac amyloidosis show grade 2 uptake (ie, a positive finding). **(B)** Review of the entire image volume revealed an incidental focus of extracardiac intense tracer uptake (arrow) in the thoracic spine. **(C)** Sagittal and **(D)** axial CT images, which were obtained from the recommended CT examination, show cortical thickening and sclerosis of the T6 vertebral body (arrow), with coarse trabecular thickening. A bone biopsy was performed, as there was concern for bone metastasis, and final histologic results coupled with serum biochemistry findings were compatible with Paget disease.

commonly in the kidney (due to physiologic excretion), followed by the bone and breast (53).

Challenges with ^{99m}Tc -PYP/DPD/HMDP Image Interpretation

False-Positive ^{99m}Tc -PYP/DPD/HMDP Scans

High blood pool activity.—By far the most common pitfall in the clinical interpretation of ^{99m}Tc -PYP/DPD/HMDP scintigraphy for suspected ATTR-CA is mistaking tracer activity in the blood pool for tracer uptake by the myocardium, resulting in a false-positive scan. ^{99m}Tc -PYP/DPD/HMDP activity in the blood pool is a frequent finding on whole-body or chest planar images, especially with 1-hour imaging. Immediately after intravenous injection, ^{99m}Tc -PYP circulates in the blood pool and is cleared from the blood by bone uptake and urinary excretion. In patients with intact renal clearance, 10% of tracer activity remains in the vascular system after 1 hour, and approximately 40%–50% of the injected dose will be taken up by the skeletal system after 1–2 hours (54). Therefore, images acquired shortly after tracer injection will show expected blood pool activity within the heart, with no

visible uptake in skeletal structures (Fig 2A). The absence of tracer uptake by the ribs is an indicator that it is too early to interpret the scan, as the tracer is still predominantly in the vascular system and has not entered and bound to the bones. The most reliable method to distinguish between blood pool activity and myocardial uptake is to repeat imaging after a delay (3 hours after injection of radiotracer), which should show clearance of blood pool activity, with clear demonstration of tracer uptake in the bones (Fig 2B). Occasionally, ^{99m}Tc -PYP activity in the blood pool may persist on the 3-hour image. The predictors of high blood pool activity are not well understood, but we encounter this more commonly in older adults or patients with renal failure. The use of SPECT and, if available, SPECT/CT imaging helps distinguish myocardial from blood pool ^{99m}Tc -PYP activity.

On planar images, ^{99m}Tc -PYP activity in the blood pool typically manifests as diffuse and amorphous uptake in the region of the heart that can be mild, moderate, or intense. True myocardial ^{99m}Tc -PYP uptake demonstrates a central clearing, best visualized on the left anterior oblique projection. The latter may be challenging to ascertain in small hearts. At SPECT imaging, positive ^{99m}Tc -PYP uptake by the

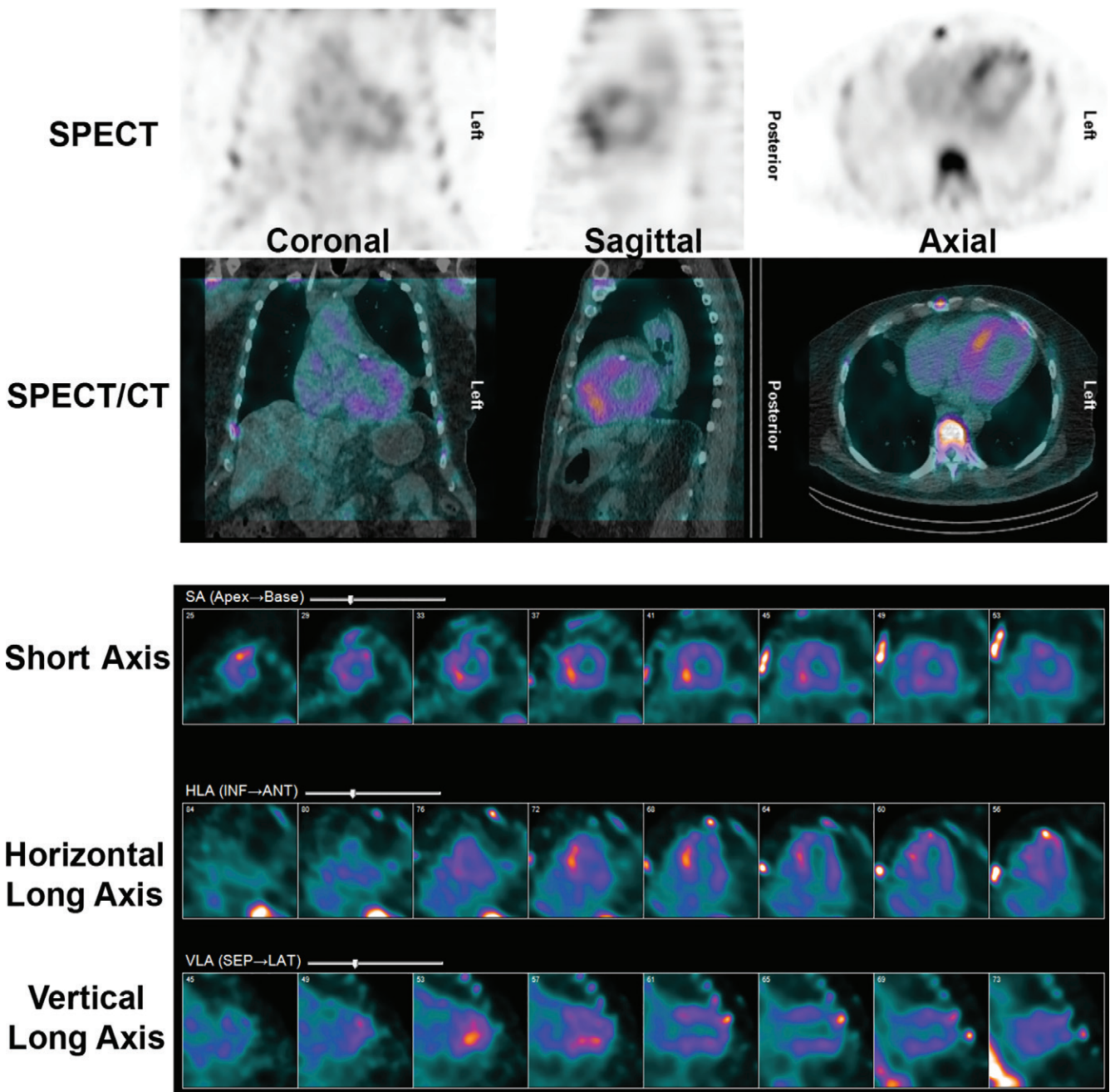


Figure 9: False-positive ^{99m} technetium pyrophosphate [^{99m}Tc-PYP] scan in a recent myocardial infarct. A 72-year-old White man underwent ^{99m}Tc-PYP SPECT/CT for evaluation of suspected transthyretin cardiac amyloidosis due to increased left ventricular wall thickening at echocardiography. His medical history was notable for an acute myocardial infarct from a thrombotic occlusion of the left anterior descending coronary artery 10 days before ^{99m}Tc-PYP SPECT/CT. The scan shows focal intense tracer uptake, most pronounced in the septum as a sequela of the recent myocardial infarction. ^{99m}Tc-PYP myocardial uptake is less specific for amyloidosis in the setting of an acute myocardial infarction and may remain positive for 6 months after infarct. ANT = anterior, HLA = horizontal long axis, INF = inferior, LAT = lateral, SA = short axis, SEP = septal, VLA = vertical long axis.

myocardial wall has an unmistakable *U* shape, or horseshoe shape, on axial and coronal images and a donut shape on sagittal images, with an appearance similar to myocardial perfusion images (Fig 3B), whereas ^{99m}Tc-PYP activity in the blood pool lacks a definite shape and is inseparable from the mediastinal activity (Fig 3A). In selected cases where blood pool activity persists on the 3-hour image and clinical suspicion remains high, further evaluation can be considered, including cardiac MRI or endomyocardial biopsy if clinically indicated.

Recent acute myocardial infarct and other myocardial injuries.—^{99m}Tc-PYP cardiac imaging was used in the 1970s for imaging acute myocardial injury from infarction (55) before it was replaced by serum cardiac biomarkers. Cell death during myocardial infarction is followed by an influx of calcium and leads to deposition of intramyocardial calcium complexes, which have high affinity for bone-avid tracers, such as ^{99m}Tc-PYP. Generally, tracer uptake in infarction is focal and localizes to an infarcted area following a typical coronary artery

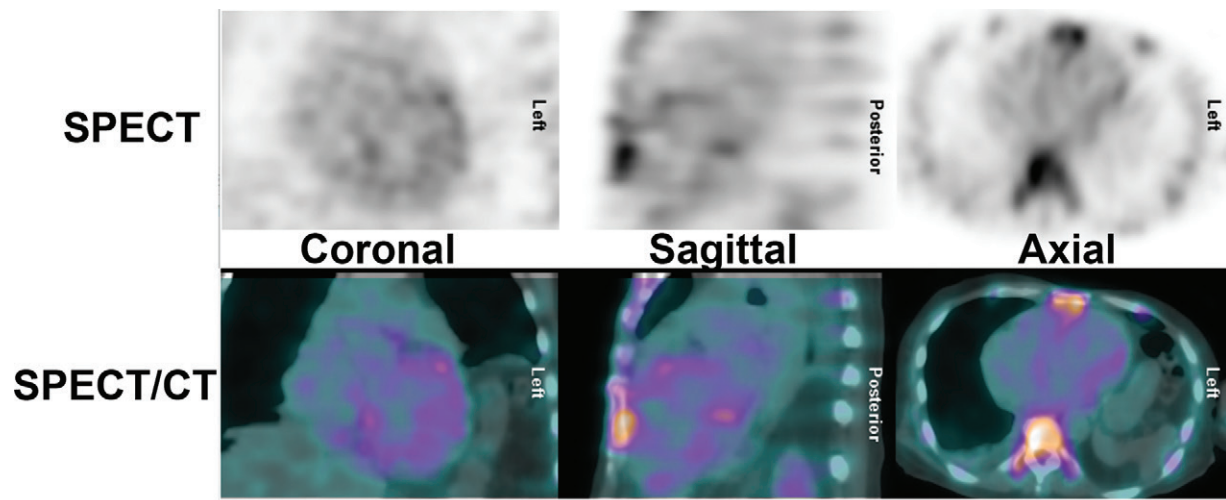


Figure 10: False-negative technetium 99m (^{99m}Tc) pyrophosphate (PYP) scan in hereditary transthyretin (ATTRv) amyloidosis. An 82-year-old African American man presented with symptoms of heart failure. Investigations revealed typical echocardiographic features of an infiltrative pathologic abnormality, and he was found to carry the Val122Ile (p.Val142Ile) transthyretin (ATTR) gene variant. His ^{99m}Tc -PYP SPECT/CT scan was, however, surprisingly, negative. The diagnosis of ATTRv cardiomyopathy was confirmed approximately 6 months later postmortem when the autopsy revealed extensive ATTR amyloid fibril deposition in the myocardium. Rarely, in patients with the Val122Ile (p.Val142Ile) variant, ^{99m}Tc -PYP scans can be negative. False-negative scans are more commonly encountered in patients with ATTRv with certain pathogenic ATTR variants, such as Phe64Leu (p.Phe84Leu) and Val30Met (p.Val50Met).

distribution. Lack of awareness of this obsolete use of ^{99m}Tc -PYP cardiac scintigraphy may lead to inappropriate timing in ordering and interpretation of the test in patients who experienced a recent acute myocardial infarction (Fig 9). Following a myocardial infarction, myocardial ^{99m}Tc -PYP uptake usually begins to diminish after 14 days as the infarcted area heals, but rarely, it may remain persistently positive beyond 6 months (56). Other instances of myocardial insult, such as myocarditis (57,58), postradiation injury (59), doxorubicin-induced cardiomyopathy (60), and hydroxychloroquine cardiotoxicity (61), have been shown in case reports to lead to diffusely increased myocardial uptake of ^{99m}Tc -PYP. Hence, it is important to note any relevant medical history that may otherwise give rise to a false-positive test result.

False-Negative ^{99m}Tc -PYP/DPD/HMDP Scans

The specificity of grade 2 or 3 uptake on ^{99m}Tc -PYP/DPD/HMDP scans combined with absence of clone is 100% for ATTR-CA, with 100% positive predictive value. This obviates endomyocardial biopsy in this group of patients. The sensitivity of a grade 2 or 3 scan for ATTR-CA is 71%, and this finding implies that almost 29% of patients with ATTR-CA have false-negative scans (12). Scans may be falsely negative in early-stage ATTR-CA disease, where amyloid infiltration is minimal (and perhaps clinically insignificant) or in patients with ATTRv amyloidosis with certain pathogenic ATTR variants, such as Phe64Leu (p.Phe84Leu) (62) and Glu61Ala (p.Glu81Ala) (63) variations. False-negative ^{99m}Tc -DPD scans are common in patients carrying Val30Met (p.Val50Met) variations with type B full-length amyloid fibrils (64), but rarely, in patients with Val122Ile (p.Val142Ile) variant, ^{99m}Tc -PYP scans can be negative (Fig 10). Therefore, in patients with high clinical suspicion of ATTR-CA but negative ^{99m}Tc -PYP/DPD/HMDP scans,

further evaluation should be considered (see section “When to Refer for Further Evaluation Including Endomyocardial Biopsy”). Note that ^{99m}Tc methyl diphosphate, a commonly used ^{99m}Tc bisphosphonate derivative for bone scintigraphy, is not recommended for imaging of cardiac amyloidosis. ^{99m}Tc methyl diphosphate has poor sensitivity for detection of ATTR-CA (11) (Fig 11).

Clinical Reporting of ^{99m}Tc -PYP/DPD/HMDP Studies

Standardized reporting of ^{99m}Tc -PYP/DPD/HMDP scans for ATTR-CA should include patient demographic characteristics and image acquisition method, documenting the type of radiotracer used, dose activity, time interval between radiotracer injection and scan acquisition, and scan technique (planar, SPECT, or SPECT/CT). Reporting of scan findings should describe visual interpretation and semiquantitative interpretation in relation to rib uptake, while reporting of H/CL ratio is optional (8). Incidental positive ancillary findings should be included as well. The conclusion should provide an overall interpretation of the findings into categories of (a) not suggestive of ATTR-CA, (b) strongly suggestive of ATTR-CA, or (c) equivocal for ATTR-CA. The report should state that evaluation for AL amyloidosis with use of serum free AL assay and serum and urine immunofixation electrophoresis is recommended in all patients undergoing ^{99m}Tc -PYP/DPD/HMDP scintigraphy for cardiac amyloidosis.

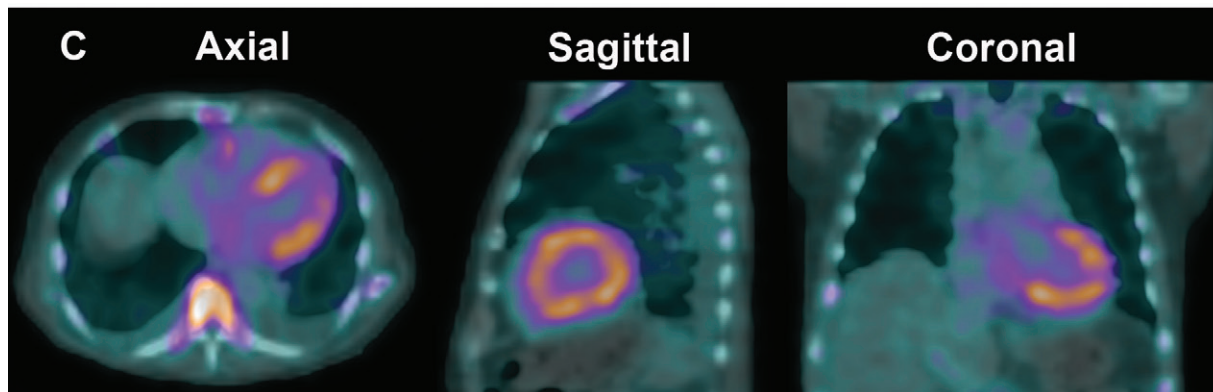
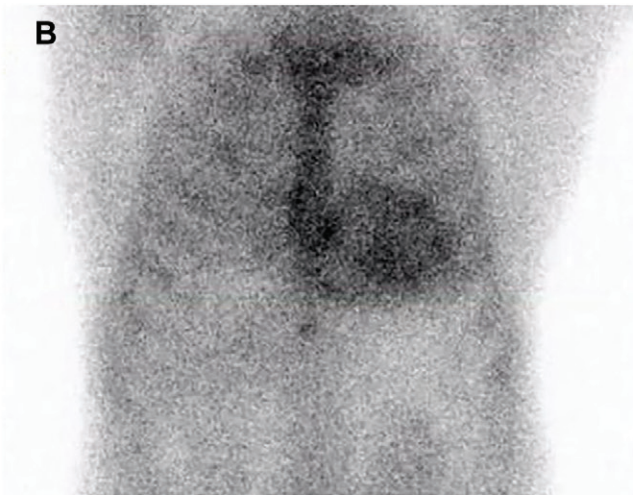
When to Refer for Further Evaluation Including Endomyocardial Biopsy

There are several reasons for further evaluation after bone-avid tracer cardiac scintigraphy. In patients with monoclonal gammopathy, the specificity of ^{99m}Tc -PYP/DPD/HMDP is

A ^{99m}Tc-MDP



Figure 11: Negative technetium ^{99m}Tc methylene diphosphonate (MDP) bone scan in transthyretin cardiac amyloidosis (ATTR-CA). **(A)** ^{99m}Tc methylene diphosphonate planar whole-body bone scan for the evaluation of bone metastasis in a 79-year-old White man with newly diagnosed malignant neoplasm reveals no abnormal focal tracer uptake suspicious for bone metastasis and no appreciable tracer uptake in the heart. **(B)** ^{99m}Tc pyrophosphate planar scan and **(C)** SPECT/CT scan obtained 30 days later for the evaluation of ATTR-CA were strongly positive.



lower, and histologic typing with mass spectrometry–based proteomic analysis of the amyloid fibrils may be necessary (12). Per data from Gillmore et al (12), grade 2 or 3 ^{99m}Tc-PYP/DPD/HMDP activity has modest sensitivity and negative predictive value for ATTR-CA. If clinical suspicion is high (eg, a gene-positive patient with typical phenotype but a ^{99m}Tc-PYP scan showing grade 0 or 1 activity), there is discordance of the imaging result. In such cases, the imaging finding may represent early ATTR-CA (if AL amyloidosis is

excluded). Management of these patients with possible early ATTR-CA is not well established and may include watchful waiting, interval ^{99m}Tc-PYP/DPD/HMDP imaging after several months, and, in select cases, endomyocardial biopsy to confirm the diagnosis (2) or initiation of targeted ATTR-CA therapy. It is advisable to refer patients with equivocal ^{99m}Tc-PYP/DPD/HMDP studies or difficult-to-interpret AL assay results to dedicated centers with high volume and multidisciplinary expertise in cardiac amyloidosis.

Table 2: Summary of the Literature on Quantitative ^{99m}Tc -PYP/DPD/HMDP SPECT and SPECT/CT Imaging

Study	Year	No. of Patients	Radiotracer	Modality and Software	Quantitative Metric	Results
Ramsay et al (67)	2018	6 with suspected ATTR-CA and 23 without ATTR-CA	^{99m}Tc -HMDP	SPECT/CT, xQUANT software	SUV _{max} of the heart, ascending aorta blood pool, and bone	SUV _{max} of 1.2 differentiates ATTR-CA from non-ATTR-CA
Caobelli et al (68)	2019	8 with clinically confirmed ATTR-CA and 5 controls	^{99m}Tc -DPD	SPECT/CT, xQUANT software	SUV _{max} and SUV _{peak} of the heart and bone	Myocardial SUV _{max} and SUV _{peak} showed a fairly strong correlation with Perugini score
Scully et al (69)	2020	100 with suspected ATTR-CA	^{99m}Tc -DPD	SPECT/CT, Hermes software	SUV _{peak} of the heart, vertebrae, paraspinal muscle, and liver; SUV retention index*	AUCs for cardiac SUV _{peak} and SUV retention index of 0.999
Wollenweber et al (70)	2020	32 with biopsy-proven or suspected ATTR-CA	^{99m}Tc -DPD	SPECT/CT, xQUANT software	SUV _{peak} of the heart, vertebra, and soft tissue; SUV _{peak} of the heart normalized to bone activity	SUV _{peak} of 3.1 has 100% sensitivity and specificity for differentiating Perugini grades 0 and 1 from 2 and 3
Dorbala et al (72)	2020	72 with biopsy-proven or suspected ATTR-CA	^{99m}Tc -PYP	SPECT/CT, MIM software	SUV _{max} , SUV _{mean} , CAA [†] , %ID	AUCs for all 4 metrics >0.96
Miller et al (66)	2021	43 with biopsy- or clinically confirmed ATTR-CA and 81 without ATTR-CA	^{99m}Tc -PYP	SPECT, FusionQuant software	CPA [‡]	AUC of 0.996; higher CPA was associated with poorer clinical outcome

Note.— ^{99m}Tc = technetium 99m, ATTR-CA = transthyretin cardiac amyloidosis, AUC = area under the receiver operating characteristic curve, CAA = cardiac amyloid activity, CPA = cardiac PYP activity, DPD = 3,3-diphosphono-1,2-propanodicarboxylic acid, HMDP = hydroxymethylene diphosphonate, %ID = percentage injected dose, PYP = pyrophosphate, SUV = standardized uptake value, SUV_{max} = maximum SUV, VOI = volume of interest.

* SUV retention index = (cardiac SUV_{peak}/vertebral SUV_{peak}) × paraspinal muscle SUV_{peak}.

† CAA = SUV_{mean} × left ventricular volume.

‡ CPA = VOI × (mean radiotracer counts of regions with abnormal myocardial activity/maximal left ventricular blood pool radiotracer activity).

Future: Quantification of Cardiac Amyloidosis with Use of SPECT and SPECT/CT

While the current methods of interpretation using visual grading are adequate for diagnosis, they are not able to fully address pertinent clinical matters, such as reliable detection of early disease, evaluation of treatment response, assessment of disease progression (65), and prognostication (24). Several groups have successfully explored the feasibility of deriving target-to-background ratios on SPECT images (66) as well as absolute quantification of cardiac technetium 99m pyrophosphate, 3,3-diphosphono-1,2-propanodicarboxylic acid, or hydroxymethylene diphosphonate uptake with use of SPECT/CT to reflect the amyloid burden in the myocardium (Table 2) (67–72). Advances in SPECT instrumentation, notably CT-based attenuation correction, scatter correction, improved recon-

struction algorithms, advanced software, as well as cadmium zinc telluride crystals, make it possible to determine standardized uptake value–based and other advanced quantitative metrics (Fig 12, Table 3) (74). Quantitative bone-avid tracer cardiac scintigraphy may have the added advantages of excellent test-retest repeatability and less interobserver variability and paves the way for application of radiomics in the evaluation of cardiac amyloidosis. Further studies are underway to validate and harmonize the process of quantification using SPECT/CT to advance it from the realm of research to clinical application.

Disclosures of conflicts of interest: Y.M.K. No relevant relationships. S.A.M.C. Research funding from Pfizer; honoraria for lectures from Ionis, BridgeBio, and Pfizer; support for travel to meetings from Ionis. V.S. Research grant from the American Society of Nuclear Cardiology (ASNC)/Pfizer; member of the Pfizer speaker bureau; unpaid member of the Society of Cardiovascular Computed Tomography and ASNC committees. R.H.F. Research funding from GlaxoSmithKline and Akcea; consulting

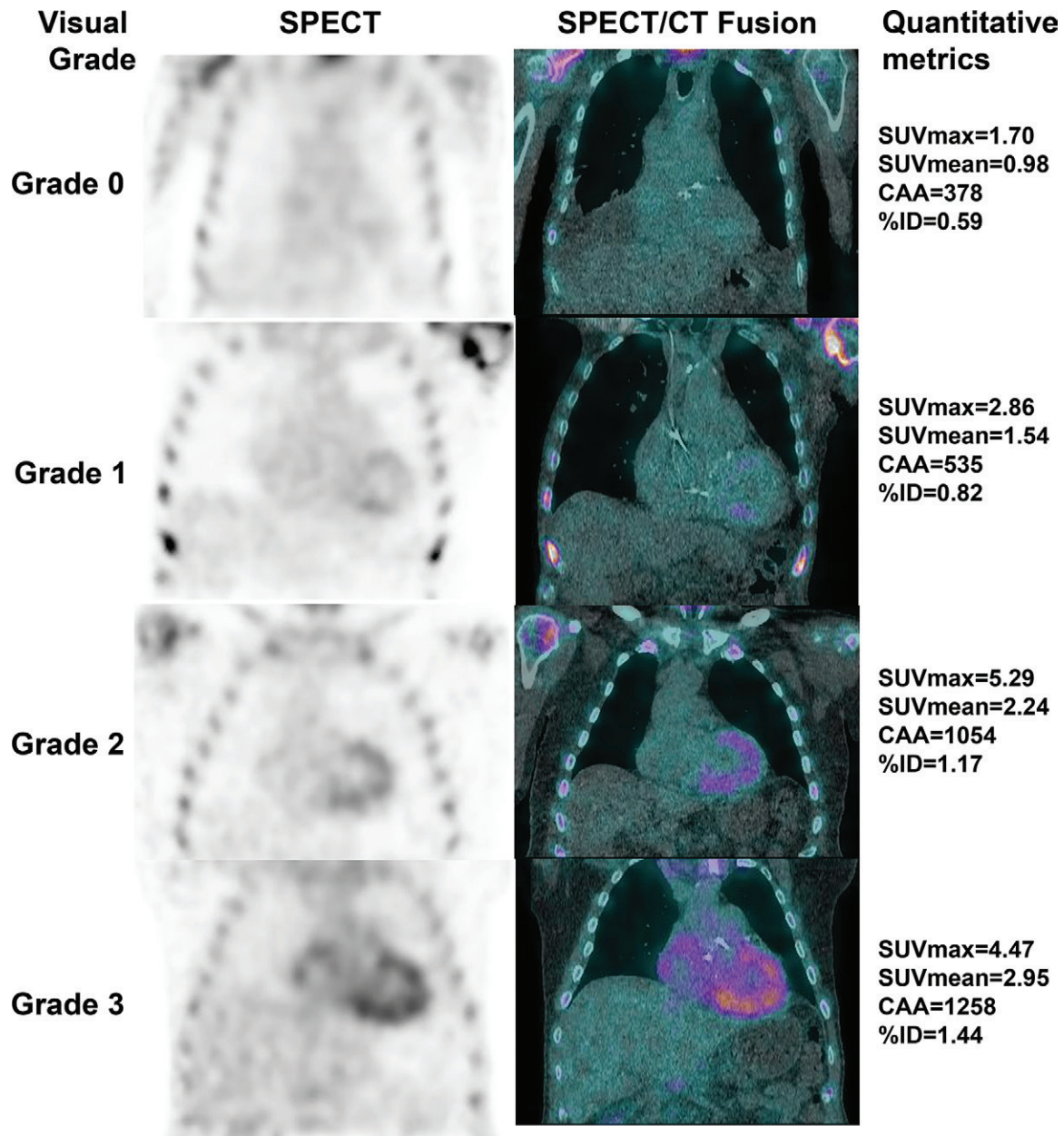


Figure 12: Visual grading and quantitative metrics from technetium 99m pyrophosphate SPECT/CT images. The left column shows attenuation-corrected SPECT images with visual grading labels; the right column shows SPECT/CT fusion images with corresponding maximum standardized uptake value (SUVmax), mean standardized uptake value (SUVmean), cardiac amyloid activity (CAA), and percentage injected dose (%ID) for each image.

fees from Ionis, Alnylam Pharmaceuticals, and Caelum Biosciences. **M.E.D.C.** Grants to institution from Gilead Sciences and Spectrum Dynamics. **S.D.** Grants to institution from Pfizer, Attralus, GE Healthcare, Philips, the National Institutes of Health, and the American Heart Association; payment for lectures from Janssen and Ionetix.

References

- Merlini G, Bellotti V. Molecular mechanisms of amyloidosis. *N Engl J Med* 2003;349(6):583–596.
- Dorbala S, Cuddy S, Falk RH. How to image cardiac amyloidosis: a practical approach. *JACC Cardiovasc Imaging* 2020;13(6):1368–1383.
- Falk RH, Alexander KM, Liao R, Dorbala S. AL (light-chain) cardiac amyloidosis: a review of diagnosis and therapy. *J Am Coll Cardiol* 2016;68(12):1323–1341.
- Kastritis E, Palladini G, Minnema MC, et al. Daratumumab-based treatment for immunoglobulin light-chain amyloidosis. *N Engl J Med* 2021;385(1):46–58.
- Ruberg FL, Grogan M, Hanna M, Kelly JW, Maurer MS. Transthyretin amyloid cardiomyopathy: JACC state-of-the-art review. *J Am Coll Cardiol* 2019;73(22):2872–2891.
- Grogan M, Scott CG, Kyle RA, et al. Natural history of wild-type transthyretin cardiac amyloidosis and risk stratification using a novel staging system. *J Am Coll Cardiol* 2016;68(10):1014–1020. [Published correction appears in *J Am Coll Cardiol* 2017;69(23):2882.]
- Quarta CC, Gonzalez-Lopez E, Gilbertson JA, et al. Diagnostic sensitivity of abdominal fat aspiration in cardiac amyloidosis. *Eur Heart J* 2017;38(24):1905–1908.
- Dorbala S, Ando Y, Bokhari S, et al. ASNC/AHA/ASE/EANM/HFSA/ISA/SCMR/SNMMI expert consensus recommendations for multimodality imaging in cardiac amyloidosis: part 1 of 2—evidence base and standardized methods of imaging. *J Nucl Cardiol* 2019;26(6):2065–2123. [Published correction appears in *J Nucl Cardiol* 2021;28(4):1761–1762.]

Table 3: Summary of Quantitative ^{99m}Tc-PYP/DPD/HMDP SPECT Metrics of Transthyretin Cardiac Amyloidosis

Metric	Definition	Units	Notes
SUV _{mean}	Tracer uptake in the VOI/(injected activity/patient weight); mean value in the VOI	g/mL	1–6; insensitive to early disease, which may start focally
SUV _{max}	Tracer uptake in the VOI/(injected activity/patient weight); maximal value in the VOI	g/mL	1–6; represents a single voxel value; can be contaminated by spillover from bone
SUV _{peak}	Highest average SUV in a 1 cm ³ or sphere or average SUV of 1 cm ³ centered on the voxel defined by SUV _{max}	g/mL	1–6; affected by region selected; can be contaminated by spillover from bone
%ID	Product of mean activity concentration in the VOI and its volume normalized to injected dose	%	6; independent of patient weight; considers myocardial volume
Retention index*	Ratio of tissue activity at time (T) to integral of plasma activity from T ₀ to T	Unitless	Need early and dynamic images to quantify this measure; challenging with later imaging tracers
Target-to-background ratio	Heart-to–contralateral lung/whole-body activity or SUV ratio; heart-to–blood pool activity or SUV ratio	Unitless	Simple to use; affected by activity in the background
Cardiac amyloid activity	Product of SUV _{mean} and LV volume	g	3, 6; considers myocardial volume
Volume of amyloid	Volume of LV myocardium above SUV threshold value	mL	6; uses a threshold SUV value; may be insensitive to early disease

Note.—1. Needs regular SPECT scanner calibration and quality control. 2. Very sensitive to VOI definition and therefore can be less repeatable. 3. Normalized to patient weight. 4. Does not consider myocardial volume. 5. Needs standardized interval between injection and scanning for comparison. 6. Affected by partial volume averaging. DPD = 3,3-diphosphono-1,2-propanodicarboxylic acid, HMDP = hydroxymethylene diphosphonate, %ID = percentage injected dose, LV = left ventricular, PYP = pyrophosphate, SUV = standardized uptake value, SUV_{max} = maximum SUV, ^{99m}Tc = technetium 99m, VOI = volume of interest. Adapted, with permission, from reference 74.

* The definition of retention index used in the article by Scully et al (69) differs from this more routine definition.

- Wizenberg TA, Muz J, Sohn YH, Samlowski W, Weissler AM. Value of positive myocardial technetium-99m-pyrophosphate scintigraphy in the noninvasive diagnosis of cardiac amyloidosis. *Am Heart J* 1982;103(4 Pt 1):468–473.
- Rapezzi C, Quarta CC, Guidalotti PL, et al. Usefulness and limitations of ^{99m}Tc-3,3-diphosphono-1,2-propanodicarboxylic acid scintigraphy in the aetiological diagnosis of amyloidotic cardiomyopathy. *Eur J Nucl Med Mol Imaging* 2011;38(3):470–478.
- Perugini E, Guidalotti PL, Salvi F, et al. Noninvasive etiologic diagnosis of cardiac amyloidosis using ^{99m}Tc-3,3-diphosphono-1,2-propanodicarboxylic acid scintigraphy. *J Am Coll Cardiol* 2005;46(6):1076–1084.
- Gillmore JD, Maurer MS, Falk RH, et al. Nonbiopsy diagnosis of cardiac transthyretin amyloidosis. *Circulation* 2016;133(24):2404–2412.
- Glaudemans AW, van Rheenen RW, van den Berg MP, et al. Bone scintigraphy with (99m)technetium-hydroxymethylene diphosphonate allows early diagnosis of cardiac involvement in patients with transthyretin-derived systemic amyloidosis. *Amyloid* 2014;21(1):35–44.
- Reimer KA, Martonoff K, Schumacher BL, Henkin RE, Quinn JL 3rd, Jennings RB. Localization of ^{99m}Tc-labeled pyrophosphate and calcium in myocardial infarcts after temporary coronary occlusion in dogs. *Proc Soc Exp Biol Med* 1977;156(2):272–276.
- Stats MA, Stone JR. Varying levels of small microcalcifications and macrophages in ATTR and AL cardiac amyloidosis: implications for utilizing nuclear medicine studies to subtype amyloidosis. *Cardiovasc Pathol* 2016;25(5):413–417.
- Martineau P, Finnerty V, Giraldeau G, Authier S, Harel F, Pelletier-Galarneau M. Examining the sensitivity of ¹⁸F-NaF PET for the imaging of cardiac amyloidosis. *J Nucl Cardiol* 2021;28(1):209–218.
- Morgenstern R, Yeh R, Castano A, Maurer MS, Bokhari S. ¹⁸Fluorine sodium fluoride positron emission tomography, a potential biomarker of transthyretin cardiac amyloidosis. *J Nucl Cardiol* 2018;25(5):1559–1567.
- Trivieri MG, Dweck MR, Abgral R, et al. ¹⁸F-sodium fluoride PET/MR for the assessment of cardiac amyloidosis. *J Am Coll Cardiol* 2016;68(24):2712–2714.
- Yang JC, Fox J, Chen C, Yu AF. Cardiac ATTR amyloid nuclear imaging—not all bone scintigraphy radionuclide tracers are created equal. *J Nucl Cardiol* 2018;25(5):1879–1884.
- Lee VW, Caldarone AG, Falk RH, Rubinow A, Cohen AS. Amyloidosis of heart and liver: comparison of Tc-99m pyrophosphate and Tc-99m methylene diphosphonate for detection. *Radiology* 1983;148(1):239–242.
- Cuscaden C, Ramsay SC, Prasad S, Goodwin B, Smith J. Estimation of prevalence of transthyretin (ATTR) cardiac amyloidosis in an Australian subpopulation using bone scans with echocardiography and clinical correlation. *J Nucl Cardiol* 2021;28(6):2845–2856.
- Fathala A. Incidentally detected cardiac amyloidosis on ^{99m}Tc-MDP bone scintigraphy. *Radiol Case Rep* 2020;15(6):705–708.
- Lin H, Zhang X, Einstein AJ, Tang G. Serial Tc-99m MDP scintigraphy demonstrating increasing cardiac uptake over time in a patient with light-chain cardiac amyloidosis. *J Nucl Cardiol* 2022;29(4):2024–2028.
- Hutt DF, Fontana M, Burniston M, et al. Prognostic utility of the Perugini grading of ^{99m}Tc-DPD scintigraphy in transthyretin (ATTR) amyloidosis and its relationship with skeletal muscle and soft tissue amyloid. *Eur Heart J Cardiovasc Imaging* 2017;18(12):1344–1350.
- Rapezzi C, Quarta CC, Guidalotti PL, et al. Role of (99m)Tc-DPD scintigraphy in diagnosis and prognosis of hereditary transthyretin-related cardiac amyloidosis. *JACC Cardiovasc Imaging* 2011;4(6):659–670.
- Castano A, Haq M, Narotsky DL, et al. Multicenter study of planar technetium 99m pyrophosphate cardiac imaging: predicting survival for patients with ATTR cardiac amyloidosis. *JAMA Cardiol* 2016;1(8):880–889.
- Mohammed SF, Mirzoyev SA, Edwards WD, et al. Left ventricular amyloid deposition in patients with heart failure and preserved ejection fraction. *JACC Heart Fail* 2014;2(2):113–122.
- Bennani Smires Y, Victor G, Ribes D, et al. Pilot study for left ventricular imaging phenotype of patients over 65 years old with heart failure and preserved ejection fraction: the high prevalence of amyloid cardiomyopathy. *Int J Cardiovasc Imaging* 2016;32(9):1403–1413.
- Devesa A, Cambor Blasco A, Pello Lázaro AM, et al. Prevalence of transthyretin amyloidosis in patients with heart failure and no left ventricular hypertrophy. *ESC Heart Fail* 2021;8(4):2856–2865.
- Lindmark K, Pilebro B, Sundström T, Lindqvist P. Prevalence of wild type transthyretin cardiac amyloidosis in a heart failure clinic. *ESC Heart Fail* 2021;8(1):745–749.
- Singal AK, Bansal R, Singh A, et al. Concomitant transthyretin amyloidosis and severe aortic stenosis in elderly Indian population: a pilot study. *JACC CardioOncol* 2021;3(4):565–576.
- Treibel TA, Fontana M, Gilbertson JA, et al. Occult transthyretin cardiac amyloid in severe calcific aortic stenosis: prevalence and prognosis in patients undergoing surgical aortic valve replacement. *Circ Cardiovasc Imaging* 2016;9(8):e005066.

33. Scully PR, Patel KP, Treibel TA, et al. Prevalence and outcome of dual aortic stenosis and cardiac amyloid pathology in patients referred for transcatheter aortic valve implantation. *Eur Heart J* 2020;41(29):2759–2767.
34. Rosenblum H, Masri A, Narotsky DL, et al. Unveiling outcomes in coexisting severe aortic stenosis and transthyretin cardiac amyloidosis. *Eur J Heart Fail* 2021;23(2):250–258.
35. Castaño A, Narotsky DL, Hamid N, et al. Unveiling transthyretin cardiac amyloidosis and its predictors among elderly patients with severe aortic stenosis undergoing transcatheter aortic valve replacement. *Eur Heart J* 2017;38(38):2879–2887.
36. Nitsche C, Aschauer S, Kammerlander AA, et al. Light-chain and transthyretin cardiac amyloidosis in severe aortic stenosis: prevalence, screening possibilities, and outcome. *Eur J Heart Fail* 2020;22(10):1852–1862.
37. Nitsche C, Scully PR, Patel KP, et al. Prevalence and outcomes of concomitant aortic stenosis and cardiac amyloidosis. *J Am Coll Cardiol* 2021;77(2):128–139.
38. AbouEzzeddine OF, Davies DR, Scott CG, et al. Prevalence of transthyretin amyloid cardiomyopathy in heart failure with preserved ejection fraction. *JAMA Cardiol* 2021;6(11):1267–1274.
39. Benson MD, Waddington-Cruz M, Berk JL, et al. Inotersen treatment for patients with hereditary transthyretin amyloidosis. *N Engl J Med* 2018;379(1):22–31.
40. Adams D, Gonzalez-Duarte A, O’Riordan WD, et al. Patisiran, an RNAi therapeutic, for hereditary transthyretin amyloidosis. *N Engl J Med* 2018;379(1):11–21.
41. Maurer MS, Schwartz JH, Gundapaneni B, et al. Tafamidis treatment for patients with transthyretin amyloid cardiomyopathy. *N Engl J Med* 2018;379(11):1007–1016.
42. Gillmore JD, Gane E, Taubel J, et al. CRISPR-Cas9 in vivo gene editing for transthyretin amyloidosis. *N Engl J Med* 2021;385(6):493–502.
43. Macedo AVS, Schwartzmann PV, de Gusmão BM, Melo MDT, Coelho-Filho OR. Advances in the treatment of cardiac amyloidosis. *Curr Treat Options Oncol* 2020;21(5):36.
44. Solomon SD, Adams D, Kristen AV, et al. Effects of patisiran, an RNA interference therapeutic, on cardiac parameters in patients with hereditary transthyretin-mediated amyloidosis: an analysis of the APOLLO study. *Circulation* 2019;139(4):431–443.
45. Fontana M, Martinez-Naharro A, Chacko L, et al. Reduction in CMR derived extracellular volume with patisiran indicates cardiac amyloid regression. *JACC Cardiovasc Imaging* 2021;14(1):189–199.
46. Treglia G, Glaudemans AWJM, Bertagna F, et al. Diagnostic accuracy of bone scintigraphy in the assessment of cardiac transthyretin-related amyloidosis: a bivariate meta-analysis. *Eur J Nucl Med Mol Imaging* 2018;45(11):1945–1955.
47. Dorbala S, Ando Y, Bokhari S, et al. Addendum to ASNC/AHA/ASE/EANM/HFSA/ISA/SCMR/SNMMI expert consensus recommendations for multimodality imaging in cardiac amyloidosis: Part 1 of 2—evidence base and standardized methods of imaging. *J Nucl Cardiol* 2021;28(4):1769–1774.
48. Love C, Din AS, Tomas MB, Kalappambath TP, Palestro CJ. Radionuclide bone imaging: an illustrative review. *RadioGraphics* 2003;23(2):341–358.
49. Hutt DF, Quigley AM, Page J, et al. Utility and limitations of 3,3-diphosphono-1,2-propanodicarboxylic acid scintigraphy in systemic amyloidosis. *Eur Heart J Cardiovasc Imaging* 2014;15(11):1289–1298.
50. Bokhari S, Castaño A, Pozniakoff T, Deslisle S, Latif F, Maurer MS. (99m) Tc-pyrophosphate scintigraphy for differentiating light-chain cardiac amyloidosis from the transthyretin-related familial and senile cardiac amyloidosis. *Circ Cardiovasc Imaging* 2013;6(2):195–201.
51. Gillmore JD, Wechalekar A, Bird J, et al. Guidelines on the diagnosis and investigation of AL amyloidosis. *Br J Haematol* 2015;168(2):207–218.
52. Phull P, Sanchowala V, Connors LH, et al. Monoclonal gammopathy of undetermined significance in systemic transthyretin amyloidosis (ATTR). *Amyloid* 2018;25(1):62–67.
53. Griffin JM, Rosenblum H, Teruya S, et al. Prevalence and significance of incidental findings on Pyp imaging in the Scan-mp study: the first 123 cases. *J Card Fail* 2020;26(10 Supplement):S34.
54. Mallinckrodt Pharmaceuticals. Technescan PYP Kit for the Preparation of Technetium Tc 99m Pyrophosphate Injection. https://www.accessdata.fda.gov/drugsatfda_docs/label/2017/018321s022lbl.pdf. Published 2017. Accessed November 26, 2022.
55. Buja LM, Parkey RW, Stokely EM, Bonte FJ, Willerson JT. Pathophysiology of technetium-99m stannous pyrophosphate and thallium-201 scintigraphy of acute anterior myocardial infarcts in dogs. *J Clin Invest* 1976;57(6):1508–1522.
56. Olson HG, Lyons KP, Aronow WS, Brown WT, Greenfield RS. Follow-up technetium-99m stannous pyrophosphate myocardial scintigrams after acute myocardial infarction. *Circulation* 1977;56(2):181–187.
57. Mitsutake A, Nakamura M, Inou T, Kikuchi Y, Takeshita A, Fujimi S. Intense, persistent myocardial avid technetium-99m-pyrophosphate scintigraphy in acute myocarditis. *Am Heart J* 1981;101(5):683–684.
58. Ahmad M, Dubiel JP. Tc-99m pyrophosphate myocardial imaging in perimyocarditis. *J Nucl Med* 1981;22(5):452–454.
59. Sojn JS, Cox JD, Youker JE, Swartz HM. Cardiac localization of 99mTc-(Sn)-pyrophosphate following irradiation of the chest. *Radiology* 1977;124(1):165–168.
60. Ziessman HA, O’Malley JP, Thrall JH. Cardiac System. In: *Nuclear Medicine: The Requisites in Radiology*. 4th ed. Philadelphia, Pa: Saunders Elsevier, 2014.
61. Chang ICY, Bois JP, Bois MC, Maleszewski JJ, Johnson GB, Grogan M. Hydroxychloroquine-mediated cardiotoxicity with a false-positive ^{99m}technetium-labeled pyrophosphate scan for transthyretin-related cardiac amyloidosis. *Circ Cardiovasc Imaging* 2018;11(1):e007059.
62. Musumeci MB, Cappelli F, Russo D, et al. Low sensitivity of bone scintigraphy in detecting Phe64Leu mutation-related transthyretin cardiac amyloidosis. *JACC Cardiovasc Imaging* 2020;13(6):1314–1321.
63. Cuddy SAM, Dorbala S, Falk RH. Complexities and pitfalls in cardiac amyloidosis. *Circulation* 2020;142(4):409–415.
64. Möckelind S, Axelsson J, Pilebro B, Lindqvist P, Suhr OB, Sundström T. Quantification of cardiac amyloid with [¹⁸F]flutemetamol in patients with V30M hereditary transthyretin amyloidosis. *Amyloid* 2020;27(3):191–199.
65. Castaño A, DeLuca A, Weinberg R, et al. Serial scanning with technetium pyrophosphate (^{99m}Tc-PYP) in advanced ATTR cardiac amyloidosis. *J Nucl Cardiol* 2016;23(6):1355–1363.
66. Miller RJH, Cadet S, Mah D, et al. Diagnostic and prognostic value of technetium-99m pyrophosphate uptake quantitation for transthyretin cardiac amyloidosis. *J Nucl Cardiol* 2021;28(5):1835–1845.
67. Ramsay SC, Lindsay K, Fong W, Patford S, Younger J, Atherton J. Tc-HDP quantitative SPECT/CT in transthyretin cardiac amyloid and the development of a reference interval for myocardial uptake in the non-affected population. *Eur J Hybrid Imaging* 2018;2(1):17.
68. Caobelli F, Braun M, Haaf P, Wild D, Zellweger MJ. Quantitative ^{99m}Tc-DPD SPECT/CT in patients with suspected ATTR cardiac amyloidosis: feasibility and correlation with visual scores. *J Nucl Cardiol* 2020;27(5):1456–1463.
69. Scully PR, Morris E, Patel KP, et al. DPD quantification in cardiac amyloidosis: a novel imaging biomarker. *JACC Cardiovasc Imaging* 2020;13(6):1353–1363. [Published correction appears in *JACC Cardiovasc Imaging* 2021;14(1):318–319.]
70. Wollenweber T, Retzl R, Kretschmer-Chott E, et al. In vivo quantification of myocardial amyloid deposits in patients with suspected transthyretin-related amyloidosis (ATTR). *J Clin Med* 2020;9(11):3446.
71. Ross JC, Hutt DF, Burniston M, et al. Quantitation of ^{99m}Tc-DPD uptake in patients with transthyretin-related cardiac amyloidosis. *Amyloid* 2018;25(3):203–210.
72. Dorbala S, Park MA, Cuddy S, et al. Absolute Quantitation of Cardiac 99mTc-Pyrophosphate Using Cadmium-Zinc-Telluride-Based SPECT/CT. *J Nucl Med*. 2021;62(5):716–722.
73. Dorbala S, Ando Y, Bokhari S, et al. Correction to: ASNC/AHA/ASE/EANM/HFSA/ISA/SCMR/SNMMI expert consensus recommendations for multimodality imaging in cardiac amyloidosis: Part 1 of 2—evidence base and standardized methods of imaging. *J Nucl Cardiol* 2021;28(4):1761–1762.
74. Dorbala S, Kijewski MF, Park MA. Quantitative bone-avid tracer SPECT/CT for cardiac amyloidosis: a crucial step forward. *JACC Cardiovasc Imaging* 2020;13(6):1364–1367.